

ADSORPTION MECHANISM(S) OF POLY(ETHYLENE OXIDE) ON  
OXIDE AND SILICATE SURFACES

By  
SHARAD MATHUR

A DISSERTATION PRESENTED TO THE GRADUATE SCHOOL OF THE  
UNIVERSITY OF FLORIDA IN PARTIAL FULFILLMENT OF THE  
REQUIREMENTS FOR THE DEGREE OF DOCTOR OF PHILOSOPHY

UNIVERSITY OF FLORIDA

1996

## ACKNOWLEDGMENTS

I would like to express my deepest gratitude to Dr. B.M. Moudgil, my major advisor, for his invaluable guidance, assistance and encouragement through this investigation.

My sincere thanks go to Dr. D.O. Shah, Dr. E.D. Whitney, Dr. C.D. Batich, Dr. H. El-Shall and Dr. R.K. Singh for serving on my supervisory committee.

To all my friends- Dr. S.Behl, Dr. R.Damodaran, N.Kulkarni, T.S. Prakash, S.Zhu, R.Kalyanraman, J. Adler and many more involved in the Materials Science and Engineering Department, I would like to express my thanks for their constructive suggestions and cheerful assistance during the course of this work. I also appreciate the experimental help rendered by Adam Bogan, Joseph Puglisi, Matt Guyot, Robert Pekrul and Andrew Gartsiewicz.

I wish to acknowledge the NSF Engineering Research Center for Particle Science and Technology at the University of Florida for providing financial support (through Grant # EEC-94-02989) and a stimulating interdisciplinary research environment.

Last, but not the least, I would like to acknowledge my wife Anuradha for her invaluable assistance during the preparation of this manuscript.

## TABLE OF CONTENTS

ACKNOWLEDGMENTS .....	ii
ABSTRACT .....	xii
CHAPTERS	
1 INTRODUCTION .....	1
Adsorption of Polymers at Solid/Liquid Interface .....	1
Polymer Adsorption .....	1
Applications .....	3
Polymer Adsorption Mechanisms .....	3
2 BACKGROUND .....	9
Introduction .....	9
Source of Isolated Hydroxyls on Dolomite .....	10
Adsorption Mechanism of PEO on Dolomite Samples .....	10
Deficiencies in the Proposed Adsorption Mechanism of PEO .....	10
Scope of the Present Study .....	13
3 EXPERIMENTAL .....	14
Materials .....	14
Oxide Samples .....	14
Silicate Samples .....	14
Polymers .....	19
Other Chemicals .....	19
Methods .....	19
Chemical Composition .....	19
Particle Characterization .....	21
PEO Characterization .....	23
Surface Chemical Characterization .....	26
AFM Studies .....	27
Flocculation Studies .....	28
Adsorption Studies .....	30
4 FLOCCULATION AND ADSORPTION STUDIES ON OXIDES .....	33
Introduction .....	33

Flocculation Studies	33
Effect of Polymer Molecular Weight	33
Effect of Dosage	33
Effect of Floc Detection Technique	36
Electrokinetic Studies	38
Effect of pH on Flocculation of Oxides with PEO	38
Adsorption Studies	45
Adsorption Kinetics of PEO on Oxides	45
Adsorption Isotherms of PEO on Oxides	45
Adsorption Mechanism of PEO	52
Effect of Negatively Charged Surface	53
Effect of Hydrated Counter-Ions	53
AFM Studies	54
Role of Specific Surface Binding Sites in PEO	
Adsorption on Silica	62
5   ROLE OF SURFACE ACIDITY OF OXIDES IN PEO ADSORPTION	63
Introduction	63
Accessibility of Surface Sites to PEO Molecules	63
Concentration of Surface Hydroxyls	64
Heat of Wetting of Oxides	66
Nature of Surface Hydroxyls	66
Point of Zero Charge of Oxides	66
Correlation between Heat of Wetting and pzc of Oxides	68
Role of Bronsted Acidity in PEO Adsorption	70
Relation Between Type of Oxide and its Point Of Zero Charge	71
Adsorption and Flocculation Behavior of $\text{MoO}_3$ and $\text{V}_2\text{O}_5$ with PEO	73
Role of Lewis Acid Sites	82
Oxide/PEO/ $\text{CCl}_4$ system	84
Hematite/Starch/Water System	84
6   CHARACTERIZATION OF PEO BINDING SITES	
ON OXIDE SURFACES	86
Introduction	86
Surface Hydroxyls on Oxides	88
Isolated Hydroxyls and PEO Adsorption	92
Effect of Heat Pretreatment	94
Adsorption of PEO on Heat Treated Samples	97
Characterization of Surface Acidity of Oxides	101
DRIFT Spectra of Adsorbed Pyridine on Oxides	101
Acidity of Silanol Groups	104

	Surface Analysis of Silica and Adsorption of PEO .....	104
	Specificity of Hydrogen-Bonding of Isolated Silanols .....	104
	Effect of pH .....	107
7	ADSORPTION AND FLOCCULATION BEHAVIOR OF SILICATES	
	WITH PEO .....	109
	Introduction .....	109
	Adsorption and Flocculation Studies .....	109
	Flocculation of Silicates .....	109
	Effect of Flocculant Dosage .....	110
	Adsorption Studies on Silicates .....	113
	AFM Studies of Adsorbed Molecules on Tremolite and Augite .....	122
	Surface Characterization of Silicate Minerals .....	135
	Correlation between Isolated Hydroxyls and Adsorption .....	138
	Adsorption Mechanism(s) of PEO on Silicates .....	140
8	CONCLUSIONS AND FUTURE WORK .....	146
	Summary .....	146
	Suggestions for Future Work .....	150
	REFERENCES .....	152
	BIOGRAPHICAL SKETCH .....	161

## LIST OF FIGURES

<u>Figure</u>	<u>Page</u>
1.1. Conformation of the adsorbed polymer molecule..	2
1.2. Schematic illustrating steric stabilization of particles.	4
1.3. Schematic of bridging flocculation of particles.	5
1.4. Schematic illustrating the selective flocculation process.	6
3.1. Crystal structures of silicate samples.	18
3.2. Size distribution of PEO samples.	25
3.3. Calibration curves for analysis of PEO in solution.	32
4.1. Flocculation behavior of oxide samples as a function of molecular weight of PEO (dosage 0.5 mg/g; pH = 9.5).	34
4.2. Flocculation behavior of oxide samples as a function of dosage of PEO of MW 8,000,000 at pH 9.5.	35
4.3. Bed volume of silica sediment as a function of PEO dosage (MW=5,000,000) at pH9.5.	37
4.4. Electrokinetic behavior of oxides as a function of pH ( $I = 0.03 \text{ kmol/m}^3$ )	39
4.5. Flocculation behavior of silica samples as a function of pH (PEO MW = 5,000,000; dosage = 0.5 mg/g).	41
4.6. Flocculation behavior of silica A as a function of PEO molecular weight at different pH (PEO dosage = 0.5 mg/g).	43
4.7. Electrokinetic behavior of silica A with and without PEO ( $I=0.03 \text{ kmol/m}^3$ )	44
4.8. Equilibrium adsorption time for PEO on oxides (PEO MW = 8,000,000; pH = 9.5).	46

4.9.	Adsorption isotherms for oxide-PEO system at pH 9.5 (PEO MW = 5,000,000) ..	47
4.10	Adsorption isotherms for oxide-PEO system at pH 3.0 (PEO MW = 5,000,000) ..	48
4.11	Adsorption isotherm of PEO (MW = 8,000,000) on silica A at pH 9.5. .	51
4.12.	AFM image of the bare silica surface. ....	55
4.13.	AFM Tapping Mode topographic image of adsorbed PEO (MW = 5,000,000 at pH 3.0) .....	56
4.14.	AFM Tapping Mode topographic image of adsorbed PEO at pH 9.5 after 1 hour of desorption. ....	58
4.15.	AFM Tapping Mode topographic image of adsorbed PEO at pH 9.5 after 2 hour of desorption. ....	59
4.16.	Effect of pH on interparticle forces between silica sphere and a flat plate with and without PEO (MW = 5,000,000). ....	61
5.1.	Schematic of Bronsted acid sites. ....	69
5.2.	Heat of wetting of oxides as a function of their point of zero charge. (After [Hea65]). ....	70
5.3.	Electrokinetic behavior of $\text{MoO}_3$ and $\text{V}_2\text{O}_5$ suspensions as function of pH. ....	75
5.4.	Adsorption isotherms of PEO on $\text{MoO}_3$ and $\text{V}_2\text{O}_5$ suspensions (PEO MW = 5,000,000; pH= 3.0). ....	76
5.5.	Saturation adsorption density of PEO (MW= 5,000,000) at pH 3.0 as a function of the point of zero charge of oxides. ....	77
5.6.	Flocculation behavior of $\text{MoO}_3$ and $\text{V}_2\text{O}_5$ as a function of molecular weight (dosage = 0.5 mg/g at pH 3.0). ....	79
5.7.	Flocculation of $\text{MoO}_3$ and $\text{V}_2\text{O}_5$ as a function of PEO dosage (pH 3.0). 80	
5.8.	Schematic showing a Lewis acid site. ....	84
6.1.	Schematic showing surface hydroxylation on various faces of anatase. 88	
6.2.	DRIFT spectra of oxides in the hydroxyl region. ....	90

6.3.	DRIFT spectra of silica B and hematite in the hydroxyl region. . . . .	91
6.4.	DRIFT spectra of heat treated silica samples. . . . .	96
6.5.	Schematic of i) amorphous silica surface showing the ring structure and ii) influence of surface curvature on H-bonding. . . . .	97
6.6.	DRIFT spectra showing effect of heat treatment on the surface hydroxylation of alumina A. . . . .	99
6.7.	Adsorption isotherms of PEO for heat treated oxides at pH 9.5 (PEO MW =5,000,000). . . . .	100
6.8.	DRIFT spectra of pyridine treated $\text{MoO}_3$ , $\text{V}_2\text{O}_5$ and $\text{SiO}_2$ samples. . . .	104
6.9.	Plot of the change in frequency of isolated silanols against the specific heat of adsorption for several vapors adsorbed on silica surface (data after [Kis65] and And [65a].. . . .	107
7.1.	Flocculation of silicates as a function of molecular weight of PEO (pH=9.5; dosage=1mg/g). . . . .	110
7.2.	Flocculation behavior of augite as a function of PEO dosage at pH 9.5. . . . .	113
7.3.	Flocculation behavior of tremolite as function of PEO dosage at pH = 9.5. . . . .	115
7.4.	Kinetics of PEO adsorption on tremolite and augite. . . . .	116
7.5.	Adsorption isotherms of PEO on chain and orthosilicates at pH 9.5 (PEO MW = 5,000,000). . . . .	117
7.6.	Adsorption isotherms of PEO on clays at pH 9.5 (PEO MW = 5,000,000). . . . .	118
7.7.	AFM image of bare tremolite surface. . . . .	124
7.8.	AFM image of adsorbed PEO on tremolite. . . . .	125
7.9.	AFM Friction image of adsorbed PEO on tremolite. . . . .	126
7.10.	Histogram of parking area of PEO molecules on tremolite. . . . .	127
7.11	AFM image of bare augite surface. . . . .	131

7.12. AFM image of adsorbed PEO on augite. ....	132
7.13. AFM Friction image of adsorbed PEO on augite. ....	133
7.14. Histogram of parking area of PEO molecules on augite. ....	134
7.15. DRIFT spectra of chain and layered silicates in the hydroxyl region. . .	137
7.16. DRIFT spectra of orthosilicate minerals in the hydroxyl region. ....	138
7.17. Adsorption of PEO on clays by interaction of the ether oxygen of PEO with the hydration shell of the exchangeable ion (Bronsted acid site). 143	

## LIST OF TABLES

<u>Table</u>	<u>Page</u>
2.1. Correlation between the intensity of the isolated hydroxyl groups on dolomite samples with flocculation and the saturation adsorption density of PEO of 5,000,000 MW [Beh93a]. . . . .	11
3.1. Oxide samples and their sources. . . . .	15
3.2. Structural Units Observed in Crystalline Silicates (After [Kin76]). . . . .	16
3.3. Silicate samples selected and their idealized chemical composition. . . . .	17
3.4. Characteristics of the Polymers used in this study. . . . .	20
3.5. Physical Characteristics of the oxide samples. . . . .	22
3.6. Physical characteristics of the silicate samples. . . . .	24
3.7. Dimensions of the flocculation cell. . . . .	29
4.1. Isoelectric Point of Oxides determined by Electrokinetic Studies. . . . .	40
4.2. Saturation adsorption density of PEO (MW = 5,000,000) on oxide samples at different pH. . . . .	49
5.1. Concentration of surface hydroxyl groups [And82]. . . . .	65
5.2. Heat of Wetting values for oxides in water [Che59; Hea65]. . . . .	67
5.3. Probable ranges of pzc of different types of oxides [Par65]. . . . .	73
5.4. Dissolution behavior of $\text{MoO}_3$ and $\text{V}_2\text{O}_5$ powders and the adsorption of dissolved ions on other oxides. . . . .	82
6.1. Surface hydroxyls on different oxides and the saturation adsorption density of PEO. . . . .	94

6.2.	Infrared bands of pyridine in the 1400-1700 $\text{cm}^{-1}$ region of the spectrum. ....	103
7.1.	Critical PEO molecular weight for flocculation of the silicate minerals at pH 9.5. ....	112
7.2.	Saturation adsorption density of PEO (MW = 5,000,000) on chain and orthosilicates. ....	120
7.3.	Estimated surface areas from Hg-porosimetry and the calculated saturation adsorption densities for tremolite and augite. ....	122
7.4.	Type of hydroxyl groups on silicates along with PEO saturation adsorption density. ....	140

Abstract of Dissertation Presented to the Graduate School  
of the University of Florida in Partial Fulfillment of the  
Requirements for the Degree of Doctor of Philosophy

ADSORPTION MECHANISM(S) OF POLY(ETHYLENE OXIDE) ON  
OXIDE AND SILICATE SURFACES

By

SHARAD MATHUR

December, 1996

Chairman: Dr. Brij M. Moudgil  
Major Department: Materials Science and Engineering

The surface modification of solids by adsorption of polymers is critical to a number of industrial processes and products. In a solvent medium, polymer adsorption on solid substrate is exploited to disperse or aggregate the particulate slurries. Solid/solid separations using selective flocculation technique rely on the specificity of the polymer for the aggregating particles. Hydrogen bonding has been suggested to be the primary adsorption mechanism for non-ionic polymers and associated with nonselectivity. However, literature survey of PEO-oxide system suggested poly(ethylene oxide) (PEO), a non-ionic polymer, to be substrate specific.

In this study the adsorption of PEO on various oxides and silicates and their flocculation behavior was systematically investigated to understand the adsorption

mechanism(s). Surface characterization of the solid substrates was performed through DRIFT, AFM, adsorption and electrokinetic measurements to identify the adsorption mechanisms. It was shown that the adsorption of PEO is substrate specific indicating that hydrogen bonding is strongly dependent on the surface chemical nature of the substrate. It was determined that strong Bronsted acid sites on the surface interact with the ether oxygen, a Lewis base, of PEO to induce adsorption and subsequently flocculation of the particles.

In the oxide/PEO system, highly acidic oxides such as  $\text{SiO}_2$ ,  $\text{MoO}_3$ , and  $\text{V}_2\text{O}_5$  strongly adsorb PEO and exhibit flocculation. On the other hand, relatively basic oxides with a point of zero charge (pzc) greater than that of silica such as  $\text{TiO}_2$ ,  $\text{Fe}_2\text{O}_3$ ,  $\text{Al}_2\text{O}_3$  and  $\text{MgO}$ , did not exhibit significant adsorption of PEO. Further, dissolved ions and charge characteristics were shown not to affect the adsorption and flocculation behavior of oxides. It was revealed for the silicate/PEO system that the connectivity of the silicate tetrahedra is essential in generation of strong Bronsted acid sites capable of interacting with PEO.

The concept of strong Bronsted sites being essential for PEO adsorption provided the commonality for the binding sites identified earlier, viz., the isolated silanols and exchangeable ions. It also showed that rather than the isolated nature of the surface hydroxyls their acid strength is of prime importance in interacting with the ether oxygen of PEO. Further, the effect of pH on adsorption of PEO and similar non-ionic polymers on silica could be explained within the framework of the established adsorption mechanism. Additionally, the results will be beneficial to identification/synthesis of selectively adsorbing polymers with applications in processing of mineral fines, controlled drug delivery systems and ultrapurification of fines.

## CHAPTER 1

### INTRODUCTION

#### Adsorption of Polymers at Solid/Liquid Interface

##### Polymer Adsorption

A flexible polymer molecule such as poly(ethylene oxide) (PEO) in solution has a dynamically changing conformation which can be described as a random coil. The size of the coil is dependent upon the solvent quality, the polymer concentration, and characteristics of the polymer chain [Spe92]. Upon adsorption of the polymer molecule at the solid solution interface, the conformation of the polymer may change from that in the solution state. The equilibrium conformation is a compromise between the enthalpic factors (which tend to maximize the segment/surface contacts) and entropic ones (trying to maintain a thick layer with many degrees of freedom). The adsorbed polymer conformation is described in terms of trains, loops and tails (see Figure 1.1). The segments bonded to the surface comprise the trains, the segments between the trains constitute the loops and the tails are the free ends of the polymer molecule. In principle, the trains, loops and tails can be distinguished by the difference in their mobility by techniques such as Small Angle Neutron Scattering, Nuclear Magnetic Resonance and Electron Spin Resonance.

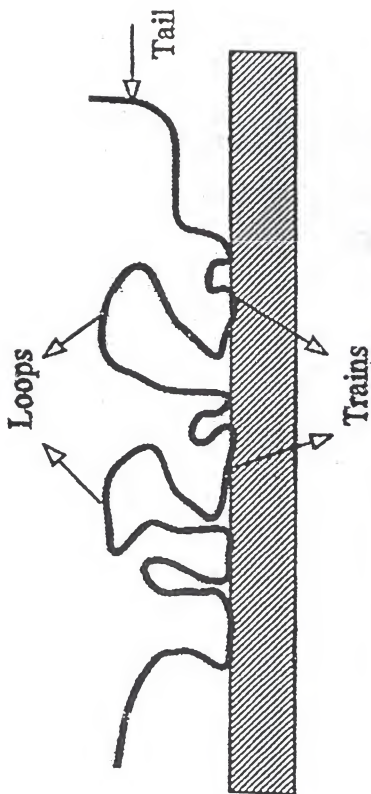


Figure 1.1. Conformation of the adsorbed polymer molecule.

### Applications

Adsorbed polymer molecules at the solid/solution interface play a very important role in many industrial and biological products and processes. For instance, polymers are used as dispersants or flocculants to stabilize or aggregate particulate slurries, respectively.

In order to disperse particles, a complete surface coverage of the polymer molecules is required in a good solvent medium so that interpenetration of the adsorbed polymer layers during interparticle collision leads to a net repulsive force. The stabilization of a suspension by this mechanism is termed as steric stabilization and is schematically illustrated in Figure 1.2. Dispersion of particles is important in ceramic and mineral processing, formulation of inks and paints, cosmetics, pharmaceutical and food industry.

A partial coating of the polymer on a particle may lead to its adsorption on a bare surface of the other colliding particle. This is the origin of bridging flocculation illustrated schematically in Figure 1.3. The flocculation of particles forms the basis for both solid/liquid and solid/solid separations. The flocculation phenomenon, when it is confined to only specific type of particles in a multi-component particulate systems is termed selective flocculation (see Figure 1.4).

### Polymer Adsorption Mechanisms

In order to optimize the effectiveness and efficiency of the polymer as a dispersant/flocculant, it is important to understand the underlying adsorption mechanism(s). This can be illustrated by way of example of the selective flocculation process. The process comprises of (1) dispersion of the fine particles

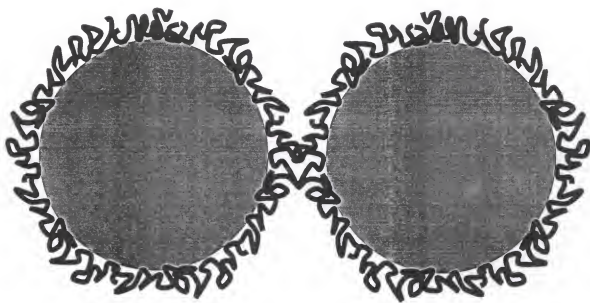


Figure 1.2. Schematic illustrating steric stabilization of particles.

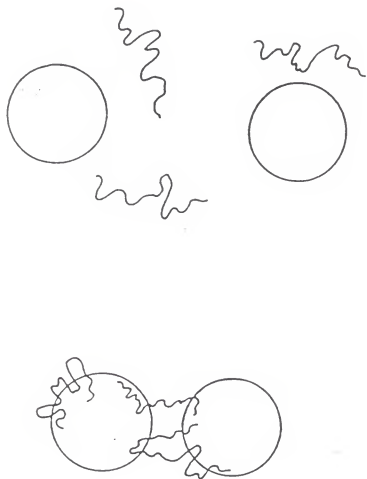


Figure 1.3. Schematic of bridging flocculation of particles.

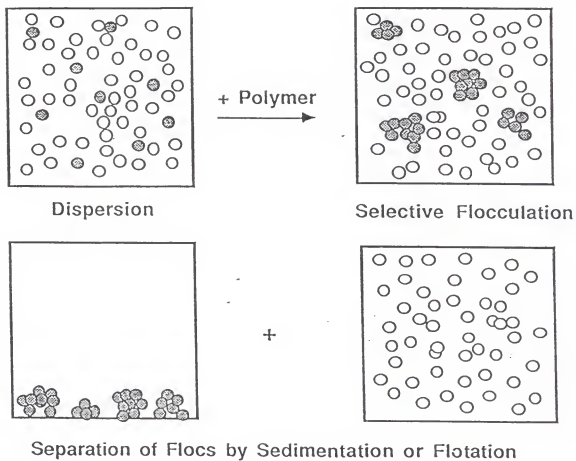


Figure 1.4. Schematic illustrating the selective flocculation process.

(2) selective adsorption of the polymer on the flocculating component and formation of the flocs, (3) floc growth which is generally achieved by conditioning at low shear, and (4) floc separation either through sedimentation/elutriation/sieving or flotation followed by cleaning of flocs by repeated redispersion and flocculation, if necessary. Among these steps, the second step, i.e., selective adsorption of the polymer is the most difficult to control and by far is the limiting step to the success of the selective flocculation technique [Att87;Mou91].

Adsorption of the polymer on a particular surface is the result of the interactions between the functional groups and the binding sites on the surface. Flocculants are high molecular weight polymers which can adsorb through a number of mechanisms such as van der Waals, electrostatic interactions, hydrogen bonding, hydrophobic interactions and chemical bonding. Clearly, the surface property chosen (hydrophobicity, hydrogen bonding, surface charge or chemical bonding) must represent the one with the greatest difference between the flocculating and non-flocculating particles.

Hydrogen bonding has been accepted as a ubiquitous mechanism for adsorption of polymers. This generalization was borne out of the fact that the oxide surfaces are rich in hydroxyl groups and the polymers contain a functional group such as the ether oxygen, or alcohol, or amide groups capable of hydrogen bonding. Recent investigations for the starch-hematite system, however, showed that the adsorption mechanism is not hydrogen bonding as was believed but a specific interaction between the Fe sites on the surface and the functional groups of the polymer [Pra91;Wei95].

The aim of the present study was to understand the adsorption mechanism(s) of PEO on oxide and silicate surfaces since the molecule was reported to adsorb onto silica [Rub76;Che85;Kil84;Kok90] and certain silicates [Sch85;Stan90;Hog85] and not on other oxides such as hematite and alumina [Kok90;Sha86]. The elucidation of the adsorption mechanism(s) of PEO was expected to provide a unifying explanation for the experimental observations documented in the literature on PEO adsorption at oxide(silicate)-solution interface. This is also expected to lead to guidelines for identification/synthesis of selectively adsorbing polymers.

## CHAPTER 2

### BACKGROUND

#### Introduction

Previous studies in the silica/PEO and silica/poly(vinyl alcohol) (PVA) systems suggested the isolated silanols to be the principal adsorption sites for PEO on silica [Rub76;Tad78;Che85;Kha88]. The extension of this concept to isolated hydroxyls was examined for the dolomite-apatite system by Behl and Moudgil [Beh93d]. The DRIFT spectra of apatite and dolomite revealed that isolated hydroxyl groups are exclusive to the dolomite A surface, whereas hydrogen-bonded hydroxyl groups are present on both apatite and dolomite surface [Beh93a]. These investigators hypothesized that any polymer capable of hydrogen bonding such as polyacrylic acid (PAA), polyacrylamide (PAM) and polyethyleneoxide (PEO) therefore should be capable of flocculating the two materials. Among these, PEO being a weak flocculant [Sch87], only the material with stronger interactions with the polymer molecules may be expected to flocculate. Experiments performed with 5,000,000 MW PEO revealed that irrespective of the amount of polymer added, flocculation of apatite was not observed. On the other hand, instantaneous flocculation of dolomite occurred justifying the assumption of a specific interaction of the ether oxygen of PEO with the isolated hydroxyls on dolomite [Beh93d].

The importance of the isolated hydroxyl groups was further shown through a correlation between their intensity on dolomite samples collected from different sources and the adsorption and flocculation with PEO (see Table 1) [Beh93d]. The dolomite samples showed similar bulk chemical composition, and it was even possible to separate one dolomite from another dolomite provided one of the dolomite could be flocculated with PEO [Mou95a].

#### Source of Isolated Hydroxyls on Dolomite

The fact that some dolomite showed the isolated hydroxyls while the others did not was unexplained [Beh93d;Mou95a]. A detailed characterization of the dolomite samples, described below, was attempted by Moudgil et al. [Mou95b] to determine the cause of the isolated OH on some dolomite samples and its absence on others. DRIFT and X-ray Diffraction (XRD) studies revealed the presence of a coating of palygorskite clay on the flocculating dolomite samples.

#### Adsorption Mechanism of PEO on Dolomite Samples

Hoghooghi [Hog85] has shown that PEO is an excellent flocculant for palygorskite. The mechanism of adsorption of PEO on dolomite A is expected to be similar to the hydrogen bonding mechanism proposed for silica. The isolated OH on dolomite A may act as proton donor in hydrogen bonding to ether oxygen of PEO.

#### Deficiencies in the Proposed Adsorption Mechanism of PEO

The correlation between saturation adsorption density of PEO and flocculation of dolomite samples with the presence of isolated hydroxyls suggested that the assumption of isolated hydroxyls being the principal adsorption sites for the

Table 2.1. Correlation between the intensity of the isolated hydroxyl groups on dolomite samples with flocculation and the saturation adsorption density of PEO of 5,000,000 MW [Beh93a].

Dolomite	Flocculation (dosage 1 mg/g)	Saturation adsorption density, mg/m <sup>2</sup>	Intensity of Isolated OH at 3619 cm <sup>-1</sup>
A	98.5	2.18	High
B	92.5	1.93	High
C	69.3	1.16	Medium
D	72.5	1.19	Medium
E	0	0.88	None
F	0	0.39	None

ether oxygen of PEO is correct. However, the presence of isolated OH on dolomite samples was determined to be due to the coating of palygorskite clay. The flocculation behavior of clays such as montmorillonite and palygorskite has been extensively studied by Scheiner and co-workers [Sch86;Sch87;Bro89]. These investigators attributed the adsorption mechanism of PEO to a hydrogen bonding mechanism involving the water shell around the exchangeable cations on the clays [Sch86;Bro89]. Although the isolated hydroxyls constitute the surface of other oxides such as alumina and hematite yet flocculation of these oxides was not observed [Kok90]. The presence of isolated hydroxyls on the surface of these oxides has been shown through vibrational spectroscopy [Hai67;Tsy72;Mor76]. Additionally, other possible mechanisms for adsorption of PEO suggested in the literature e.g. electrostatic interactions with a positively charged surface, and complex binding with adsorbed ions such as  $K^+$ ,  $Cd^+$ ,  $Mg^+$  etc. [Bai76; Kje81; Ana87; Beh93d;Pra95] have not been examined in detail to explain the flocculation behavior of various oxides with PEO.

Thermodynamically, the overall free energy of the polymer adsorption process must be negative. In addition to the enthalpic factors such as the segment/surface and water-surface interactions the overall entropy changes associated with the adsorption process are also important. In fact, the lack of PEO adsorption on alumina and hematite was suggested to be due to the lack of accessibility of PEO molecules to the surface sites [Kok90]. The entropy factor was earlier invoked by Greenland to explain the unreactivity of aluminol and silanol groups with PVA [Gre72a,b]. Thus the adsorption mechanism(s) need to consider

the entropy contribution to polymer adsorption. Further, the adsorption mechanism(s) must also be consistent with the observed decrease in adsorption of non-ionic polymers, such as PEO and PVA, with pH [Rub76;Che85;Tad78;Kha88].

In order to further understand the adsorption mechanism of PEO and similar non-ionic polymers, a systematic study involving surface-chemical characterization of various oxides and different types of silicates was undertaken. The reason for selecting a variety of substrates was to examine all the possible mechanisms reported in the literature including the accessibility factor, and establish the predominant mechanism of PEO adsorption on oxides and silicates.

#### Scope of the Present Study

The specific objectives of the present investigation are as follows:

1. Establish the mechanism(s) of PEO adsorption on oxides. Specifically, it is proposed to understand the role of different type of surface sites in interaction with the ether oxygen of PEO.
2. Examine the effect of pH on adsorption of non-ionic polymers such as PEO.
3. Evaluate the role of surface accessibility in polymer adsorption.
4. Examine the adsorption mechanism(s) of PEO on mixed oxides such as silicates based on better understanding of the same on simple oxides.

## CHAPTER 3

### EXPERIMENTAL

#### Materials

##### Oxide Samples

The oxide samples along with their sources are listed in Table 3.1. These were selected so as to encompass a range of acidic to basic surfaces. The oxide samples were used as received except  $V_2O_5$  and Silica B which were wet ground to obtain -400 mesh ( $<38\ \mu\text{m}$ ) fraction.

##### Silicate Samples

The silicate samples chosen were representative of the different classes of silicates. The characteristic structural features of these classes are summarized in Table 3.2. The minerals selected and their idealized chemical compositions are listed in Table 3.3. Although the Si/O ratio in palygorskite is 2.75, which is characteristic of the amphiboles, the arrangement of the chains is such that the clay is considered to be a pseudo-layered silicate [Gri68]. The crystal structures of the silicate samples are shown in Figure 3.1. The as received samples from Ward's Natural Establishment Inc., NY, were crushed in a Chipmunk crusher and then pulverized and subsequently sieved to yield different size fractions. The -400 mesh fraction of the silicate samples was used in this study.

Table 3.1. Oxide samples and their source.

Oxide Sample	Code	Source
Silica	(A)	Geltech Inc., FL
	(A)	IMC- Agrico, FL
Titania		Alfa
Hematite		Alfa
Alumina	(A)	Sumitomo
	(B)	Alcoa
Magnesia		Mallingcrockdt
Molybdenum Oxide		Alfa
Vanadium Oxide		Alfa

Table 3.2. Structural Units Observed in Crystalline Silicates (After [Kin76]).

Oxygen-Silicon Ratio	Silicon-Oxygen Groups	Structural Units	Type
2	$\text{SiO}_2$	Three dimensional Network	Framework
2.5	$\text{Si}_4\text{O}_{10}$	Sheets	Layered
2.75	$\text{Si}_4\text{O}_{11}$	Chains	Amphiboles
3.0	$\text{SiO}_3$	Chains	Pyroxenes
4.0	$\text{SiO}_4$	Isolated orthosilicate tetrahedra	Orthosilicates

Table 3.3. Silicate samples selected and their idealized chemical composition.

Material	Type of silicate	Chemical Formula
Palygorskite	Layer	$(\text{OH}_2)_4(\text{OH})_2\text{Mg}_5\text{Si}_8\text{O}_{22} \cdot 4\text{H}_2\text{O}$
Kaolinite	Layer	$\text{Al}_2\text{Si}_4\text{O}_{10}(\text{OH})_2$
Tremolite	amphibole	$\text{Ca}_2\text{Mg}_5[\text{Si}_8\text{O}_{22}](\text{OH})_2$
Augite	pyroxene	$(\text{Ca},\text{Na})(\text{Mg},\text{Fe},\text{Al})(\text{Si},\text{Al})_2\text{O}_6$
Almandite	orthosilicate	$\text{Fe}_3\text{Al}_2\text{Si}_3\text{O}_{12}$
Topaz	"	$\text{Al}_2(\text{SiO}_4)(\text{OH})$
Olivine	"	$(\text{Mg},\text{Fe})_2\text{SiO}_4$

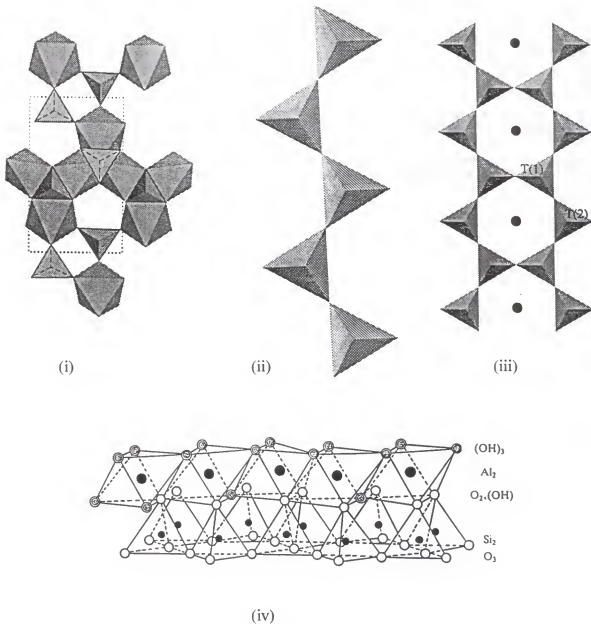


Figure 3.1. Crystal structures of silicate samples: (i) isolated  $\text{SiO}_4$  tetrahedra as in almandine, olivine and topaz, (ii)  $\text{SiO}_4$  chain in pyroxene, augite, (iii) double  $\text{SiO}_4$  chains in amphibole, tremolite and (iv)  $\text{SiO}_4$  layer in kaolinite.

### Polymers

Poly(ethylene oxide) (PEO) of different molecular weights along with the source and calculated radius of gyration is listed in Table 3.4. These samples were used as received.

### Other Chemicals

All experiments were conducted in distilled water (DI) of specific conductivity less than 1  $\mu\text{mho/cm}$ . Potassium hydroxide (KOH) and nitric acid ( $\text{HNO}_3$ ) used as pH modifiers were obtained from Fisher Scientific Co. Pyridine, used as a probe molecule for characterization of the surface acidity, was also procured from Fisher Scientific Co.

### Methods

#### Chemical Composition

The as received oxide samples were specified to be of more than 99.9% purity. Silica A was prepared by the sol-gel technique (Stober silica) while silica B was electrostatically separated from the fluorapatite and acid washed to remove the minor phosphate impurity. The  $\text{P}_2\text{O}_5$  content of the silica B sample was below the detection limit (0.05 wt.%) of the Perkin Elmer II inductively coupled plasma (ICP) spectrometer. Alumina B was determined by ICP to contain, on weight basis, 99.9%  $\text{Al}_2\text{O}_3$ , 0.01%  $\text{SiO}_2$ , 0.02%  $\text{Fe}_2\text{O}_3$  and 0.07%  $\text{Na}_2\text{O}$ .

The silicates samples were characterized for the purity primarily by the hydroxyl band of their DRIFT spectra. No quantitative analysis of the samples was attempted.

Table 3.4. Characteristics of the Polymers used in this study.

Source	Molecular Weight	Radius of Gyration, $R_g$ (nm)
Polysciences, Inc.	8,000,000	177
Polysciences, Inc.	5,000,000	144
Polysciences, Inc.	4,000,000	126
Aldrich	900,000	52
Polysciences, Inc.	600,000	41
Polysciences, Inc.	1,00,000	14
Polysciences, Inc.	18,500	6

### Particle Characterization

All the oxide and silicate powders were characterized for particle size distribution and surface area.

#### Oxides

Particle size distribution. The particle size distribution of the oxide samples was determined using Micromeritics X-ray Sedigraph 5100 and the characteristic diameters are presented in Table 3.5. It is observed that silica A is monodisperse. The silica A particles are spherical in shape, which is a characteristic of the Stober process to synthesize silica. Silica B,  $\text{MoO}_3$  and  $\text{MgO}$  particles are coarser than the other oxide samples.

Surface area. The surface area was essential to compare the adsorption density of PEO on different substrate. The size of the high molecular weight PEO is such that the BET method is insensitive to the corresponding pore size, e.g., 288 nm for 5,000,000 MW PEO molecule. The specific surface area of the oxide samples was, therefore, determined by mercury porosimetry (Micromeritics Autopore III 9420) and the results are presented in Table 3.5.

In mercury porosimetry the raw data generated for a powder sample consists of the intrusion volume of mercury versus the applied pressure. The interparticle pores are filled first and the slope of the graph changes at the point when the intraparticle pores on the surface are intruded by the mercury. The pore radius and corresponding surface area are calculated from the assumption of a cylindrical geometry of the pore. The calculated surface area for non-porous spherical particles of silica A ( $1\mu\text{m}$ ) is  $2.85\text{ m}^2/\text{g}$  which is in good agreement with the

Table 3.5. Physical Characteristics of the oxide samples

Sample	Average Particle Size, $\mu\text{m}$			Specific Surface Area, $\text{m}^2/\text{g}$
	$d_{16}$	$d_{50}$	$d_{84}$	
$\text{SiO}_2$ (A)	$1 \pm 0.1$			3.18
$\text{SiO}_2$ (B)	2.4	8.5	18.0	1.91
$\text{TiO}_2$	0.1	0.3	0.5	11.10
$\text{Fe}_2\text{O}_3$	0.3	0.6	1.5	8.23
$\text{Al}_2\text{O}_3$ (A)	0.2	0.5	0.8	7.11
$\text{Al}_2\text{O}_3$ (B)				
MgO	0.8	1.7	6.8	3.38
$\text{MoO}_3$	3.1	6.4	8.2	1.33
$\text{V}_2\text{O}_5$	0.2	0.6	1.0	7.13

experimental value of  $3.18 \text{ m}^2/\text{g}$ . Similarly, the size distribution of the other oxide samples and the surface area values indicate that the particles are essentially non-porous.

### Silicates

Particle size distribution. The particle size distribution of the ground -400 mesh fraction ( $< 38 \mu\text{m}$ ) of tremolite and augite determined by Micromeritics X-ray Sedigraph 5100 is shown in Table 3.6. It is revealed that the silicate particles are coarser than the oxide samples.

Surface area. The specific surface area of the silicate minerals was determined by Autosorb Micromeritics ASAP 2000 system. The surface area was estimated by the BET method using adsorption and desorption of nitrogen and is presented in Table 3.6. The relatively higher specific surface areas for tremolite and augite indicate that the samples have a significant amount of porosity associated with them. The Hg-porosimetry, as in the case of the oxides, was, therefore, used to determine the effective surface area for PEO adsorption for tremolite and augite.

### PEO Characterization

The PEO samples received were granular in appearance and the molecular weight specified by the manufacturer is an average value. In order to determine the polydispersity of the high molecular weight fractions light scattering on PEO solutions was performed using Brookhaven BI 90. The size measured is the hydrodynamic diameter ( $2xR_g^z$ ) of the polymer molecules in solution. The results presented in Figure 3.2 reveal that the polymers are polydisperse in nature.

Table 3.6. Physical characteristics of the silicate samples.

Sample	Average Particle Size, $\mu\text{m}$			Specific Surface Area, $\text{m}^2/\text{g}$	
	$d_{16}$	$d_{50}$	$d_{84}$	Hg-P*	BET
Tremolite	6.0	11.0	32.0	3.51	13.88
Augite	5.0	15.0	30.0	3.51	4.11
Kaolinite	< 38.0			-	15.52
Palygorskite				-	117.0
Almandite				-	0.79
Olivine				-	1.33
Topaz				-	4.54

Hg-P\* = mercury porosimetry

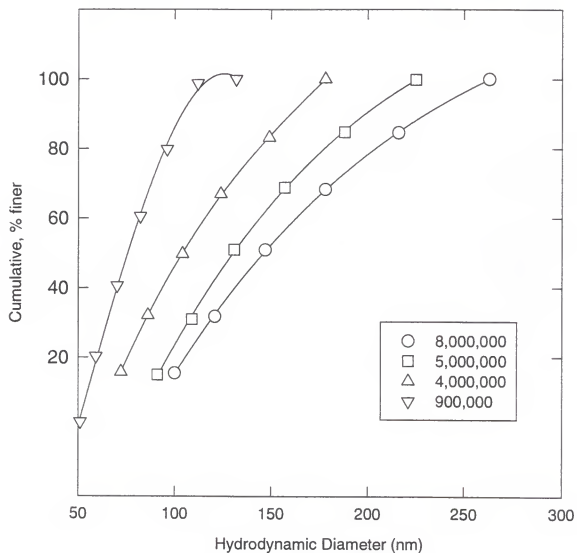


Figure 3.2. Size distribution of PEO samples. The molecular weights are indicated in the legend.

### Surface Chemical Characterization

The determination of the adsorption mechanism of PEO involved a knowledge of the surface chemical groups and charge characteristics of the samples.

### Infrared studies

Samples used for FT-IR analysis were prepared by mixing a 0.05g of vacuum dried sample with about 0.75 g of potassium bromide (KBr). The mixture was then filled in a sample cup mounted on a diffuse reflectance stage. The IR spectra was taken using a Nicolet 740 spectrometer. The beam was aligned for every sample to yield a maximum signal and the baseline was adjusted using the software. The evolution of the DRIFT spectra as a function of temperature was performed on Nicolet 60SX spectrometer using the heating stage.

The acidity of the surface chemical groups on the oxides was probed by pyridine adsorption which involved soaking 1g of the sample in 25 ml liquid pyridine for 1 hour. The samples were air-dried under a fumehood and subsequently kept in a vacuum oven at 60°C for 12 hours. The samples were then mixed with KBr prior to obtaining the DRIFT spectra.

### Electrokinetic studies

Zeta potential of the oxide samples was measured using the Laser Zee Meter (Pen Kem Model 501) to determine their isoelectric point. 50 mg of the powder sample was suspended in 100 ml of .03 kmol/m<sup>3</sup> KNO<sub>3</sub> solution except for MoO<sub>3</sub> and V<sub>2</sub>O<sub>5</sub> which exhibited ionic strength in excess of .03 kmol/m<sup>3</sup>.

For these two oxides, the centrifuged suspension from a 2 wt.% slurry was used as such to determine the zeta potential of the suspended solids. The Laser Zee Meter was also used to determine the zeta potential of PEO coated silica samples.

### AFM Studies

The Atomic Force Microscope (AFM) studies were conducted to characterize the conformation of the adsorbed polymer layer at the solid/solution interface. The samples were imaged in a liquid cell where the suspension conditions such as the pH and ionic strength can be simulated. The samples used for the AFM study were as-received fused silica plates from Herasil Amereus and polished samples of augite and tremolite rocks which were received from Ward's Natural Establishment Inc., NY. The final polishing of the silicate samples was done using 0.03  $\mu\text{m}$  iron oxide suspension from Buehler.

The AFM was used in both the contact and tapping modes to image the microstructure at the solid solution interface. The interpretation of the images was facilitated by the image analyzer software of the AFM.

The contact mode was also used to obtain force/distance profiles between a glass sphere of 10-40  $\mu\text{m}$  diameter attached to the cantilever and the fused silica plate with and without the adsorbed polymer. These profiles were obtained by suspending the x-y raster motion of the piezoelectric and measuring the deflection of the cantilever as it approached the surface. The cantilever used had a force constant of 0.30 N/m. Thus the measured deflection values were converted to the corresponding force values as a function of the separation distance.

### Flocculation Studies

These were conducted to macroscopically evaluate the effect of PEO adsorption on the particles.

### Flocculation apparatus

The flocculation of particulate suspensions has been shown to be sensitive to the type of agitation used [Hog85]. Hence it is necessary to maintain uniform, hydrodynamic conditions in all the flocculation experiments. The mixing unit employed in this study is based on the standard tank design [Dir81].

The dimensions of the mixing tank are listed in Table 3.7. A 150 ml beaker fitted with removable plexiglas baffles of appropriate dimensions was used for flocculation tests. A stainless steel turbine impeller with four blades mounted on a variable speed motor was employed to agitate the sample.

### Flocculation procedure

Material suspension of pulp density 2g/100 ml was prepared in DI water and aged for one hour. The maximum pH variation after aging was determined to be 0.2 pH units. After aging, the suspension was agitated at 1100 rpm, for 240 seconds while the pH was adjusted to the desired value. The suspension was sonicated for 30 seconds at a setting of 50 W to ensure complete dispersion, and a pre-determined amount of PEO was added. The agitation was continued at 1100 rpm for 120 seconds within which the flocculation was observed to be complete. The formation of flocs was evaluated in a sedimentation column while the quantification of floc formation was obtained via floc separation over a 400 mesh screen.

Table 3.7. Dimensions of the flocculation cell.

Flocculation Cell Part	Dimension, cm
Tank diameter	6.2
Impeller height from tank bottom	0.5
Impeller blade width	1.6
Liquid height	4.6
Baffle width	4.0

### Polymer Solution Preparation

Polymer solutions were prepared by mixing 0.25 g granular polymer with 500 ml DI water to yield a 500 ppm solution. The solution was stirred for 16h at 500 rpm and covered to avoid exposure to ultraviolet radiation which decomposes the polymer. The polymer solution was prepared fresh every day for the experiments since changes were observed in PEO adsorption when stored for more than one day [Mou92].

### Adsorption Studies

These were conducted to measure the affinity of the surface for the PEO molecules. The adsorption isotherms, in conjunction with the knowledge of the surface chemical groups, provided insight into the adsorption mechanism of PEO on oxide and silicate surface.

Adsorption was carried out by contacting the polymer solution with 2 wt.% solids in 100 ml solution in 150 ml beakers (same as the flocculation tank). Sixteen beakers were simultaneously stirred on a 16-pad magnetic stirrer at 500 rpm. The equilibrium time for adsorption was first determined by studying the kinetics of polymer adsorption with a high polymer dosage (10mg/g solids or 200 ppm). After equilibration the sample was centrifuged at 15,000 rpm for 10 minutes and the supernatant withdrawn. The residual PEO in the solution was determined by Total Organic Carbon (TOC) analyzer. Adsorption was determined by the solution depletion method. The saturation adsorption density, which is the maximum possible amount of polymer on the surface, was obtained by fitting Langmuir equation for high concentrations [Att91, Beh93].

### PEO Analysis

The amount of residual polymer in the supernatant was determined using the TOC (Shimadzu). Calibration curves were obtained for PEO of MW 5,000,000 and 8,000,000 by using standard solutions of PEO (see Figure 3.3) and correcting the measured values for the initial carbon content in the supernatant. The inorganic carbon was minimized by acidifying the PEO solutions with 85 wt.% phosphoric acid and sparging the solution with carbon-free air from gas cylinder. The concentration value measured had a cumulative variance of less than 1%.

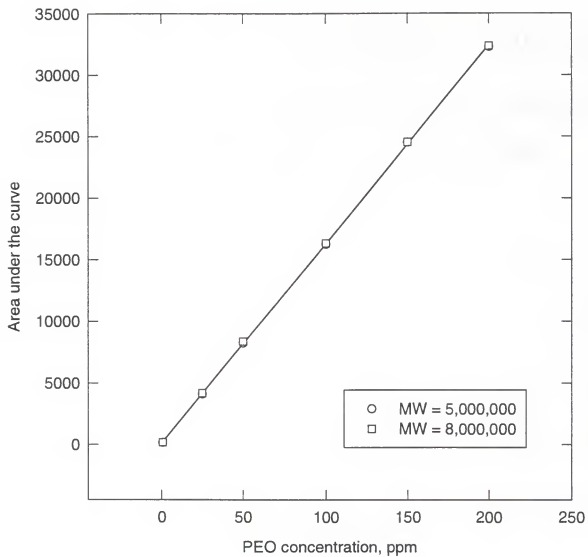


Figure 3.3. Calibration curves for analysis of PEO in solution.

## CHAPTER 4

### FLOCCULATION AND ADSORPTION STUDIES ON OXIDES

#### Introduction

In this Chapter the flocculation behavior of common oxides such as silica, titania, hematite, alumina and magnesia with PEO and the related adsorption studies are discussed to identify the underlying adsorption mechanism(s).

#### Flocculation Studies

##### Effect of Polymer Molecular Weight

The adsorption of a relatively high molecular weight polymer on the substrate generally implies the possibility of floc formation. However, there exists a critical molecular weight beyond which one can detect flocculation [Beh93a]. At lower molecular weight the polymer may act as a dispersant.

The flocculation behavior of all the oxides as a function of the molecular weight of PEO at 0.5 mg/g dosage is shown in Figure 4.1. It is observed that irrespective of the molecular weight of PEO no flocculation of any oxide except silica A is observed. The critical molecular weight of PEO at which flocculation of silica A occurred was found to be 8,000,000.

##### Effect of Dosage

It is observed from Figure 4.2 that silica flocculation exhibits a maximum as a function of PEO dosage, whereas the other oxides did not flocculate in the dosage

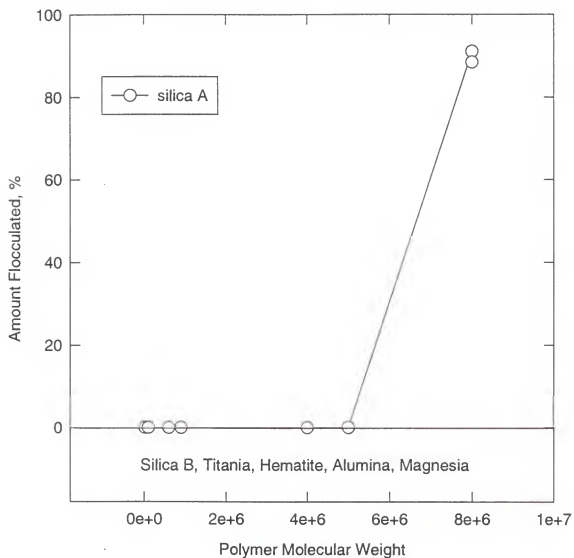


Figure 4.1. Flocculation behavior of oxide samples as a function of the molecular weight of PEO (dosage = 0.5 mg/g; pH = 9.5).

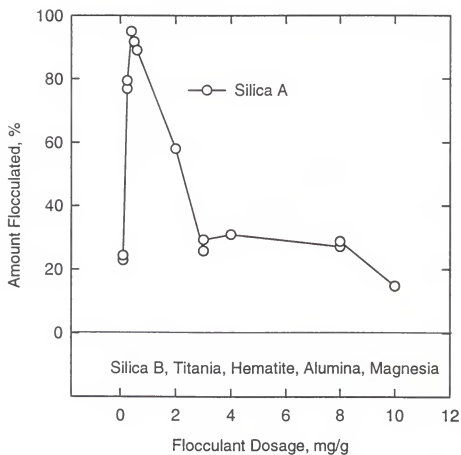


Figure 4.2. Flocculation behavior of oxide samples as a function of dosage of PEO of MW 8,000,000 at pH 9.5.

range examined. The existence of a maximum in flocculation followed by restabilization is in agreement with the bridging mechanism of flocculation. In silica-PEO system a similar flocculation behavior with dosage has been reported in the past by Rubio and Kitchener [Rub76] and Cheng [Che 85] with PEO of 5,000,000 MW.

#### Effect of Floc Detection Technique

It must be noted that silica particles are 1  $\mu\text{m}$  in size and flocs are separated using a 400 mesh (37 $\mu\text{m}$ ) screen. It is, therefore, likely that smaller flocs formed with a lower molecular weight flocculant may not be detected by sieving. Thus, determination of the critical molecular weight is strongly influenced by the floc detection technique.

In order to observe flocculation with 5,000,000 MW PEO settling tests were conducted on silica A and the results are shown in Figure 4.3. It is seen that the trend of bed volume with dosage is similar to that shown in Figure 4.2 indicating floc formation in the system. Koksai et al [Kok90] and Shah [Sha86] reported no measurable flocculation of hematite and alumina with PEO using settling tests to detect the onset of flocculation.

The lack of flocculation of silica B at pH 9.5 is not unexpected. Koksai et al [Kok90] observed the flocculation of quartzite only near the isoelectric point of 2.5 while no flocculation was detected beyond pH 4.0. Rubio and Kitchener [Rub76] observed that the precipitated silica was virtually non-flocculable at higher than pH 8.0 while the heat treated silica was only slightly flocculated when the pH was raised to 9.5 from 2.0. Cheng [Che85] also observed an enhanced flocculation of silica

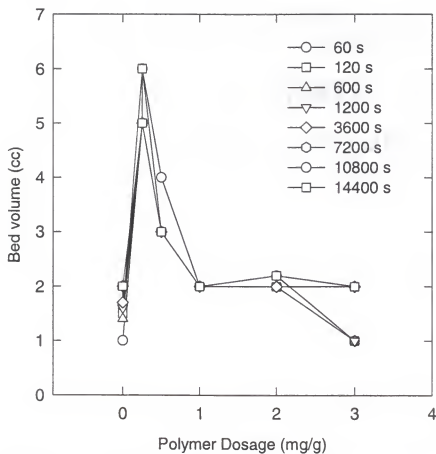


Figure 4.3. Bed volume of silica sediment as a function of PEO dosage (MW = 5,000,000) at pH = 9.5.

at pH 3.7. Thus flocculation of silica B is expected near its isoelectric point and this may be true for the other oxides.

### Electrokinetic Studies

The electrokinetic behavior of the oxide samples is summarized in Figure 4.4. The measured isoelectric point (iep) values summarized in Table 4.1 are in agreement with the literature values [Ree92].

### Effect of pH on Flocculation of Oxides with PEO

The effect of pH on flocculation of the silica samples with PEO of 5000,000 MW is shown in Figure 4.5. In accordance with previous work flocculation of both the silica samples in the acidic pH range was observed. Further, a sharp decrease in flocculation beyond pH 3.0 was noticed indicating a decrease in the adsorption of PEO on negatively charged surfaces. In fact, when the pH of the flocced slurry of silica B was raised to 9.5 the flocs begin to disappear and a dispersed suspension of silica particles was obtained.

Flocculation of oxides other than silica was not observed in the pH range 2.5-10.0. The non-flocculation of hematite and alumina in this pH range was also reported by Koksai et al [Kok90]. This implies that neither neutral sites such as MOH (which are a maximum at the isoelectric point) nor positively charged sites such as  $\text{MOH}_2^+$  (which predominate below the isoelectric point) lead to adsorption of PEO on these oxides. Further, silica A flocculated when it exhibited a high negative charge, and both silica samples flocculated near the isoelectric point. Thus electrokinetic characteristics of an oxide sample do not necessarily govern the adsorption of PEO.

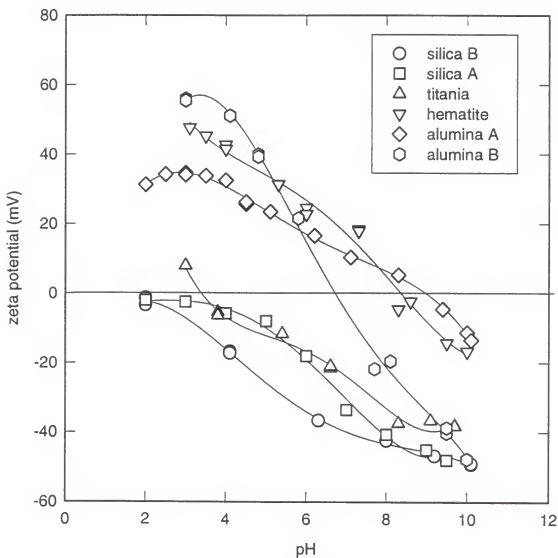


Figure 4.4. Electrokinetic behavior of oxides as a function of pH ( $\text{KNO}_3 = 0.03 \text{ kmol/m}^3$ ).

Table 4.1. Isoelectric Point of Oxides determined by Electrokinetic Studies

Oxide	Isoelectric Point
Silica A	2.0
Silica B	2.0
Titania	3.8
Hematite	8.4
Alumina A	8.8
Alumina B	7.4
Magnesia	-

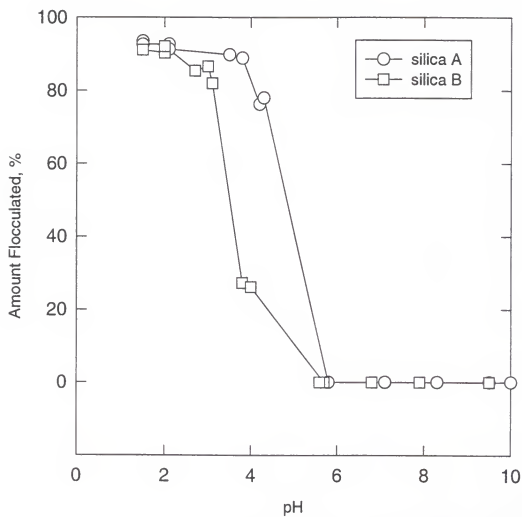


Figure 4.5. Flocculation behavior of silica samples as a function of pH (PEO MW = 5,000,000; dosage = 0.5 mg/g).

The critical molecular weight of PEO for flocculation of silica A shifted to 900,000 from 8,000,000 when the pH was decreased from 9.5 to 3.0 (see Figure 4.6). Assuming the adsorption behavior of PEO to be similar at both pH values the increase in flocculation of silica particles with decrease in pH may be attributed to the reduction in the zeta potential of the silica surface allowing a closer approach between the particles. In such a case it is only with PEO of 8,000,000 MW that the zeta potential is expected to be significantly low at pH 9.5 due to the adsorbed layer exceeding a critical thickness of the order of the thickness of the order of the thickness of the electrical double layer ( $110 \text{ nm}$  at  $I=10^{-5} \text{ kmol/m}^3$ ).

The electrokinetic data for silica A with and without adsorbed PEO of 18,500 MW is plotted in Figure 4.7. It is indicated that the adsorbed layer thickness of the 18,500 MW PEO is sufficient to result in a zero zeta potential. Thus a decrease in the zeta potential is not the reason for a decrease in the critical molecular weight of PEO for flocculation of silica suspensions with increase in pH. Rubio and Kitchener [Rub76] and Cheng [Che85] showed that the saturation adsorption density of PEO on silica decreases with increase in pH. A direct correlation between flocculation and saturation adsorption density was suggested by Behl and Moudgil [Beh93] for adsorption of PEO on several dolomite samples. Adsorption studies were therefore undertaken to explain the flocculation behavior of the different oxide samples and identify the PEO adsorption mechanism(s).

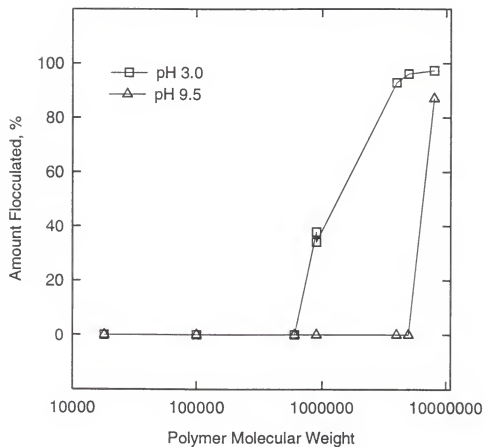


Figure 4.6. Flocculation behavior of silica A as a function of PEO molecular weight at different pH (PEO dosage = 0.5 mg/g).

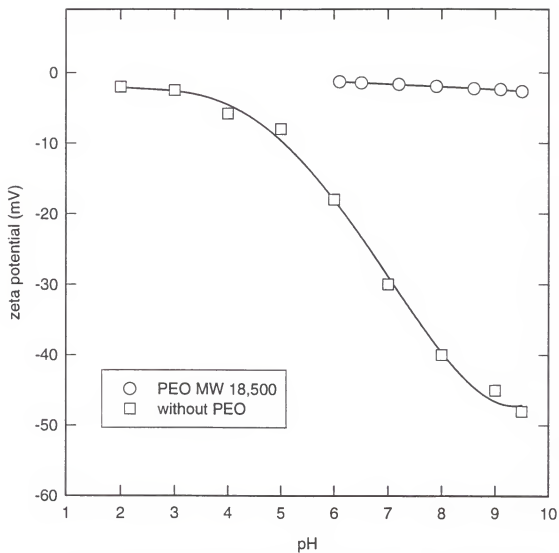


Figure 4.7. Electrokinetic behavior of silica A with and without PEO ( $I=0.03 \text{ kmol/m}^3$ ).

## Adsorption Studies

### Adsorption Kinetics of PEO on Oxides

The adsorption kinetics of PEO of 8,000,000 MW on the different oxide samples were examined and the results are presented in Figure 4.8. It is observed that equilibration is achieved in about 4 hours for silica A while the remaining samples did not exhibit any adsorption of PEO even after 24 hours. Thus further adsorption tests were performed with an equilibration time of 4 hours.

### Adsorption Isotherms of PEO on Oxides

The adsorption isotherms for all the oxide samples at pH 9.5 and 3.0 with PEO of 5,000,000 MW are plotted in Figures 4.9 and 4.10 respectively. The saturation adsorption density of PEO on various oxides under the two pH levels is summarized in Table 4.2. Considering that an equivalent monolayer of PEO corresponds to a saturation adsorption density of  $0.4 \text{ mg/m}^2$  it is clear that oxides other than silica did not exhibit significant surface coverage by PEO.

It is observed from Figures 4.9 and 4.10 that in contrast to silica A PEO adsorption on silica B was significantly affected by pH. The notable effect of pH on adsorption of PEO on silica is indicative of the flocculation behavior of the silica suspensions described in Figures 4.2 and 4.5. Although the saturation adsorption density of PEO on silica A is significant with 5,000,000 MW it is 25% lesser at the higher pH indicating a lesser number of the active sites and hence a lower probability for flocculation at pH 9.5 according to the equivalent site concept proposed by Behl and Moudgil [Beh93c]. Thus larger flocs were obtained only in the acidic pH range and not at pH 9.5 (see Figure 4.5). However, with 8,000,000

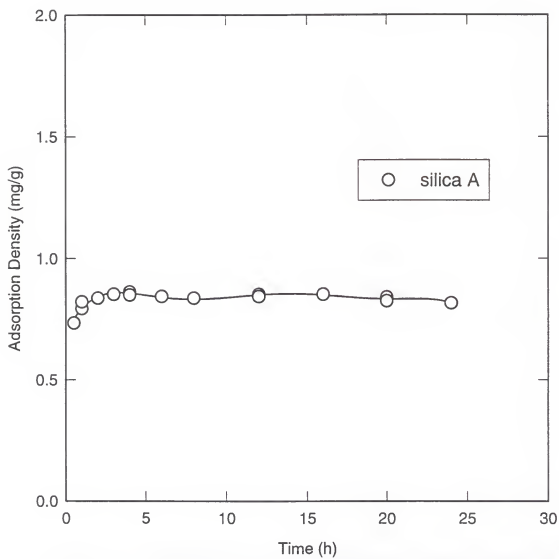


Figure 4.8. Equilibrium adsorption time for PEO on oxides (PEO MW = 8,000,000; pH 9.5).

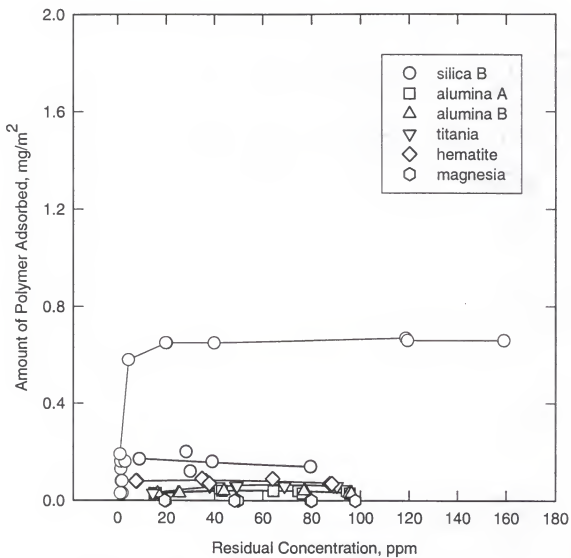


Figure 4.9. Adsorption isotherms for oxide-PEO system at pH 9.5 (PEO MW = 5,000,000).

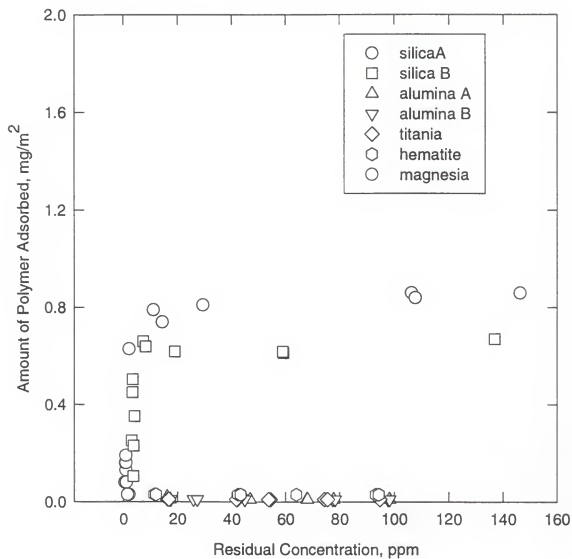


Figure 4.10. Adsorption isotherms for oxide-PEO system at pH 3.0 (PEO MW = 5,000,000).

Table 4.2. Saturation adsorption density of PEO (MW = 5,000,000) on oxide samples at different pH.

Oxide	Saturation Adsorption Density, mg/m <sup>2</sup>	
	pH 3.0	pH 9.5
Silica A	0.80	0.65
Silica B	0.63	0.17
Titania	< 0.1	
Hematite		
Alumina A		
Alumina B		
Magnesia		

MW PEO large flocs were observed at pH 9.5 indicating the adsorption to be similar to that obtained at pH 3.0 with 5,000,000 MW PEO. The saturation adsorption density of 8,000,000 MW PEO at pH 9.5 from the isotherm in Figure 4.11 was determined to be  $0.8 \text{ mg/m}^2$  which is similar to that obtained for 5,000,000 MW PEO at pH 3.0 (see Table 4.2).

The saturation adsorption density of  $0.8 \text{ mg/m}^2$  of PEO on silica A is twice that of the equivalent monolayer adsorption density. Fleer et al [Fle83] and Blaakmeer [Bla90] have suggested that the saturation adsorption is about 2 to 5 times the equivalent monolayer, primarily due to compaction of the polymer molecule at high adsorption densities. The maximum in flocculation of silica A at pH 9.5 is observed at about  $0.16 \text{ mg/m}^2$  adsorption density ( $0.4 \text{ mg/g}$  dosage) with both 5,000,000 and 8,000,000 MW PEO (see Figures 4.2 and 4.3). The occurrence of maximum in floc formation at less than half the surface coverage ( $0.2 \text{ mg/m}^2$ ) may be attributed to the polydispersity of the polymer [Beh93b].

Adsorption studies for PEO/oxide system besides silica have been reported only for alumina. The negligible adsorption of 5,000,000 MW PEO on alumina was earlier shown by Shah [Sha86]. In a recent study of adsorption behavior of 8000 PEG on oxides and silicates it was shown that the adsorption of PEO on alumina was negligible [Wal96]. The presence of impurity ions such as sodium on alumina B also did not influence the adsorption results when it is well known that sodium ions complex with PEO in solution [Ana87; Bai76; Pra95] indicating that complexation with adsorbed surface ions is not a mechanism for PEO adsorption.

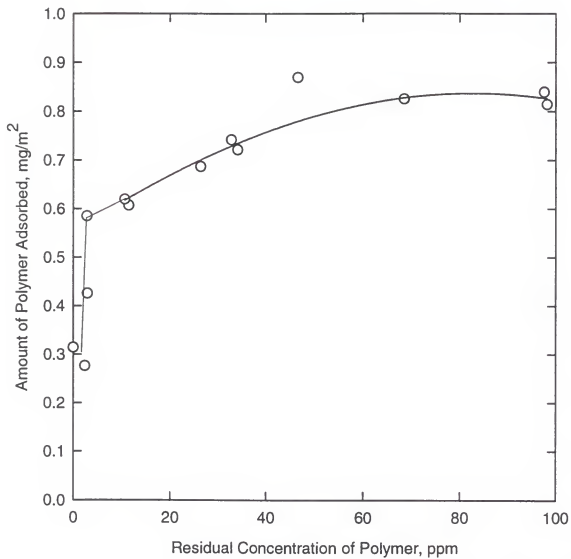


Figure 4.11. Adsorption isotherm of PEO (MW = 8,000,000) on silica A at pH 9.5.

### Adsorption Mechanism of PEO

It has been shown so far that positively charged sites ( $\text{MOH}_2^+$ ) or adsorbed ions which complex with ether oxygen in solution, and electrostatic considerations do not play a major role in the PEO adsorption process. Rubio and Kitchener [Rub76] suggested the following possible adsorption mechanisms of PEO on silica to explain the effect of pH.

1. Increased repulsion of PEO from an increasingly negatively charged interface as the pH is increased. This is because the ether oxygen with the two lone pair of electrons is considered to be slightly negatively charged. Thus the effect of surface ionization is through a general double-layer phenomenon rather than the loss of binding sites. The evidence in support of this explanation was the slight increase in PEO adsorption at a given pH with electrolyte addition.
2. The binding sites for the ether oxygen of PEO are the surface hydroxyls on the solid surface. It has been shown by infra-red studies that hydroxyls of different acid strength are present on the silica surface. The chemical characteristics of the surface hydroxyls have been shown to vary and it is possible that the most readily dissociable silanol group, i.e., the most acidic group are the most important one for adsorption of PEO. These sites are thus ionized first as the pH is increased leading to decreased adsorption of PEO.
3. Hydrated counter-ions prevent PEO from approaching the surface as the negative charge increases with the pH. This hypothesis was also suggested

by Iler [Ile75] who showed that incorporation of aluminosilicate anions into the silica surface enabling it to retain a negative charge in the acidic solution led to a decrease in flocculation.

#### Effect of Negatively Charged Surface

The non-adsorption of PEO on oxides other than silica at their isoelectric points indicates that explanation (1) above probably plays a minor role in adsorption of PEO. The repulsion of PEO molecule from a negatively charged silica surface resulting in decreased adsorption upon increase in pH implies that a positively charged surface should attract PEO which was found not to be the case as oxides below their iep did not exhibit significant adsorption of PEO. Also, electrokinetic studies showed that silica A possesses a similar charge as silica B at any pH yet their adsorption behavior is very different.

The evidence provided by Rubio and Kitchener [Rub76] in favor of the electrostatic interactions is the slight increase in PEO adsorption with electrolyte addition. There is about 10% increase in saturation adsorption for precipitated silica in the presence of 0.02 M NaCl. Similarly, Cheng [Che85] also observed a 10% increase in adsorption of PEO with 0.02 M NaCl. Addition of NaCl up to 1 M strength to non-flocculating oxide suspensions, however, did not result in any measurable adsorption of PEO indicating that repulsion from a highly negative charged surface is not a major reason for non-adsorption of PEO.

#### Effect of Hydrated Counter-Ions

The hypothesis of hydrated counter-ions preventing the approach of PEO molecules to the surface at higher pH assumes that the binding sites remain intact.

This implies that the adsorption of PEO at higher pH can be realized by contacting silica particles at a lower pH close to the isoelectric point and then increasing the pH. This hypothesis was experimentally observed at the solid/solution interface with the aid of AFM.

### AFM Studies

Imaging of Adsorbed PEO Layer using Tapping Mode. The tapping mode of the AFM was used to image the adsorbed PEO molecules at i) pH 3.0 and (ii) pH 9.5 by injection of 50 ppm of 5,000,000 MW PEO. In a separate experiment the initial pH was first maintained at 3.0 then changed to 9.5 and the desorption process observed. The AFM image of the bare silica plate is shown in Figure 4.12 with the average surface roughness determined to be less than 2 nm.

The AFM image of the adsorbed polymer layer at pH 3.0 is presented in Figure 4.13. The thickness of the molecules was determined to vary from 25-40 nm which can be attributed to the polydisperse nature of the PEO molecules. The hydrodynamic thickness of adsorbed homopolymers on a saturated surface in a good solvent has been predicted to be between  $2-3 R_g$  [deG 81; deG 82; Sch82]. In the present case it thus seems that the probe did not detect the hydrodynamic thickness of the PEO molecules since the  $R_g$  of the PEO molecule of 5,000,000 MW is 144nm.

Photon Correlation Spectroscopy (PCS) measurements for the latex-PEO system has shown that for PEO molecular weight greater than 280,000 the hydrodynamic thickness is more than  $2 R_g$  [Coh84;Cos84]. In the same system, Cosgrove et al [Cos84], however, found that Small Angle Neutron Scattering

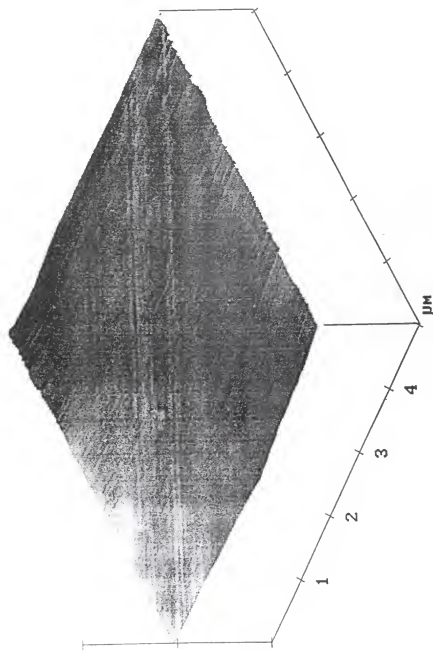


Figure 4.12. AFM image of bare silica surface.

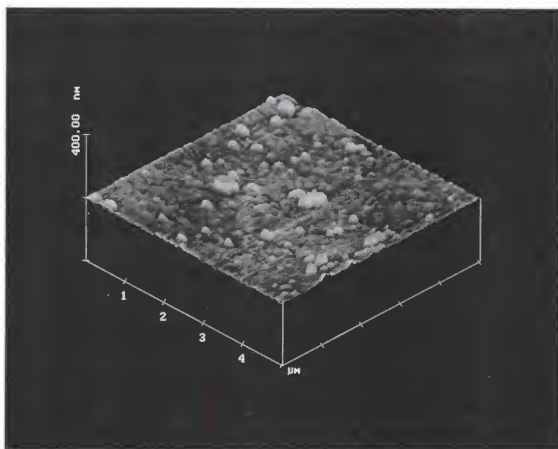


Figure 4.13. AFM Tapping Mode topographic image of adsorbed PEO (MW= 5,000,000 at pH 3.0)

(SANS) grossly underestimated the adsorbed layer thickness. The thickness of PEO molecule of 660,000 detected by SANS was found to be only 15 nm whereas with PCS a thickness of 95 nm was calculated. They attributed this discrepancy to detection of the segment density distribution of only the trains and loops and not of the tails by SANS. The segment density distribution of the adsorbed polymer has been shown to decrease exponentially with distance from the solid/solution interface [Cos84]. Thus a significantly lower thickness may be detected if the probe is not sensitive to the periphery of the adsorbed layer.

The image of the adsorbed polymer molecules at pH 9.5 after an hour of pH change is shown in Figure 4.14. A much lower adsorption density of polymer molecules on the surface is observed. The image after another hour is similar to that of the virgin surface except a few isolated patches (see Figure 4.15). This, is the first reported direct proof of desorption of polymer molecules of high molecular weight upon pH change.

It has been argued that at any given instant the probability that all the attached segments detach from the surface is so low that the adsorption for all practical purposes can be considered to be irreversible. However, de Gennes has pointed out the fallacy in this argument and showed that desorption is possible [deG87]. The desorption in the present study cannot be attributed to dilution since the polymer concentration was always maintained at 50 ppm. Further, the polymer was already adsorbed so that the possibility of inaccessibility to the surface due to the presence of hydrated counter-ions does not arise. The only reason which can then account for PEO desorption with increasing pH is the loss of binding sites for the ether oxygen of PEO.

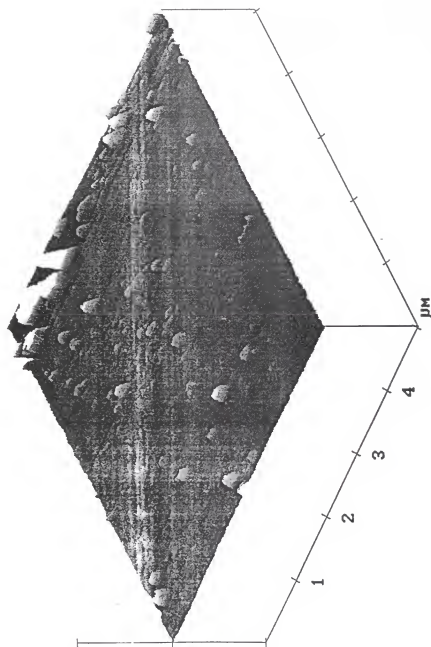


Figure 4.14. AFM Tapping Mode topographic image of adsorbed PEO at pH 9.5 after 1 hour of desorption.

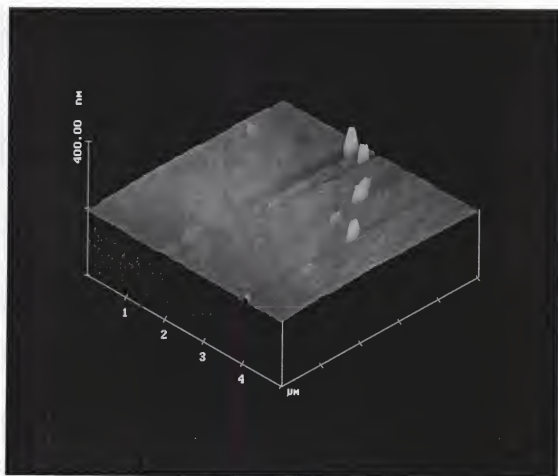


Figure 4.15. AFM Tapping Mode topographic image of adsorbed PEO at pH 9.5 after two hours of desorption.

Force/Distance profiles with Contact Mode. The adsorption of PEO on the silica plate at pH 3.0 and its desorption at pH 9.5 was corroborated in the AFM studies by obtaining force/distance profiles using a glass sphere attached to the AFM cantilever. The results presented in Figure 4.14 indicate that at pH 3.0, in the absence of PEO, the net interaction profile does not show the presence of a repulsive force, as expected from the electrokinetic considerations and the DLVO theory. However, in the presence of PEO a steric repulsive force is observed revealing the adsorption of the polymer. On the other hand, at pH 9.5, the force/distance profiles remain virtually unchanged with and without the PEO indicating the absence of an adsorbed layer.

The onset of the steric repulsion was observed at about 100 nm (see Figure 4.16). Thus the thickness of the adsorbed layer is estimated to be about 50 nm on each surface which is an underestimate with respect to the predicted and observed values in latex/PEO system [deG81; deG82; Sch82; Coh84; Cos84]. However, as mentioned above, the detection of the hydrodynamic thickness is dependent upon the sensitivity of the measuring probe to the peripheral layers of the adsorbed polymer. The measurement of force distance profiles to estimate the adsorbed layer thickness has been shown to be insensitive to the outer regions of the adsorbed polymer layer [Luc90]. Luckham and Klein [Luc90] measured the onset of repulsive interactions between adsorbed PEO layers (MW = 1,200,000) on mica in Surface Force Apparatus (SFA) at 190 nm. However, the thickness of the adsorbed PEO layer (95 nm) is about the  $R_g$  (86 nm) of the PEO molecule. Further, these investigators have shown the effect of incubation time on the measured force/distance profiles. Measurements after only 1 hour of polymer

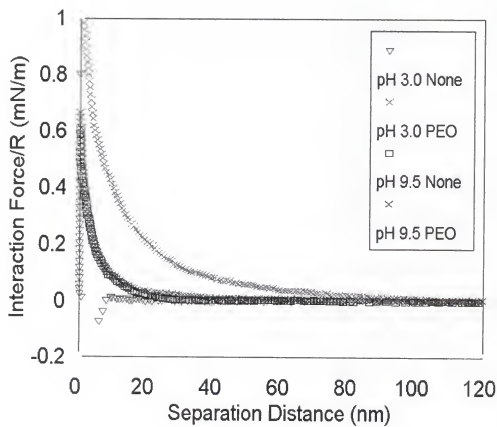


Fig 4.16. Effect of pH on interparticle forces between silica sphere and a flat plate with and without PEO(MW = 5,000,000).

contact time with the mica surfaces indicated the onset of interaction at 20 nm while after 16 h this value was found to be 190 nm. This behavior is not clear at present and further studies are needed to resolve this issue. An incubation time of 1 hour in the present case may, therefore, be responsible for a lower thickness of the adsorbed layer.

#### Role of Specific Surface Binding Sites in PEO Adsorption on Silica

It is clear from the AFM studies that there are specific PEO binding sites present on the silica plate at pH 3.0 which are lost when the pH is increased to 9.5. These are probably the most acidic silanol groups which dissociate at higher pH leading to the ionization of the site to a negatively charged species and loss of the bond with the ether oxygen. The ionization of the binding site to a negatively charged species is corroborated by the electrokinetic data (see Figure 4.4) and the force/distance profiles (see Figure 4.16).

A similar mechanism was proposed by Evans and Napper [Eva73] to explain the decrease in PEO adsorption with increasing pH for the latex/PEO system. The binding sites on the latex were carboxylic acid groups which at low pH participated in hydrogen bonding with the ether oxygen of PEO. The ionization of the acid sites led to the loss of PEO adsorption at higher pH.

It is also observed that the adsorption behavior of PEO as a function of pH on silica plate used in the AFM resembles that of silica B. The relative insensitivity of PEO adsorption on silica A to pH is in contrast to the behavior on silica B and silica plate and may be related to a different distribution of acidic sites and will be examined in Chapter 6. The lack of PEO adsorption on certain oxides which is not clear yet is discussed first in Chapter 05.

## CHAPTER 5

### ROLE OF SURFACE ACIDITY OF OXIDES IN PEO ADSORPTION

#### Introduction

In the last Chapter it was shown that no oxide other than silica exhibited significant adsorption of PEO. The mechanism of PEO adsorption on silica, consistent with the effect of pH, was indicated to involve the acidity of surface sites. In this Chapter this concept is discussed further to understand the reasons for lack of adsorption of PEO on other oxides.

Koksal et al [Kok90] suggested that the lack of adsorption of PEO on alumina and hematite was due to the inaccessibility of the surface adsorption sites to PEO molecules. This explanation was found to be inconsistent with the effect of pH on PEO adsorption on silica in Chapter 4. The reason advanced by Koksal et al [Kok90] for the inaccessibility to the surface sites of PEO molecules, however, was not the hydrated counter ions but entropic factors which are discussed next.

#### Accessibility of Surface Sites to PEO Molecules

The net free energy change associated with the polymer adsorption must be negative and involves changes in both enthalpic and entropic factors. In the case of the oxides the processes contributing to the entropy changes on PEO adsorption are: i) the loss of water from the oxide surface, ii) loss of conformational entropy of the PEO molecule due to attachment of segments to the surface which were otherwise mobile and the iii) the entropy of dilution of the bulk phase.

The ether oxygen itself has three water molecules attached to it and they have been shown not to detach in solution when PEO complexes with various ions [Pra95]. The presence of the hydration layer has been demonstrated on  $\text{SiO}_2$ ,  $\text{TiO}_2$ , and  $\text{Al}_2\text{O}_3$  through measurement of hydration forces attributed to this layer [Gra93]. The disintegration of the hydration layer will be favored since it will result in more degrees of freedom for the water molecules along with dilution of bulk water. However, if the loss of conformational entropy of the polymer exceeds the gain in entropy by the loss of hydrated water molecules then the adsorption process is not favorable. In such a case, the surface sites will remain inaccessible to the polymer molecules. The replacement of water molecules on the surface is related to the concentration of the hydroxyl groups since these provide the adsorption sites for water molecules.

#### Concentration of Surface Hydroxyls

The concentration of surface hydroxyl groups on oxides has been determined by several investigators and is summarized in Table 5.1 [And82]. It is clear that alumina, hematite and titania are more hydrated than the silica surface and therefore release of water molecules is more favored from their surfaces. Thus the lack of PEO adsorption on alumina, hematite and titania does not seem to be due to entropic reasons. Koksall et al [Kok90], however, suggested that stronger hydrogen bonding of water molecules to the surface hydroxyls on hematite and alumina prevents the interaction of PEO with the latter. In such a case favorable entropy changes for PEO adsorption are expected to be affected the most for

Table 5.1. Concentration of surface hydroxyl groups [And82].

Oxide	Number of OH/nm <sup>2</sup>
Silica	4.2-5.1
Titania	4.9-6.2
Hematite	4.6-9.1
Alumina	15

hydrated oxides such as alumina and hematite. The argument of Koksai et al [Kok90] for stronger hydrogen bonding between the water molecules and surface hydroxyls was based on the number of surface hydroxyls per unit area and not on the energetics of water-surface hydroxyl interaction. Further, some overlap of the hydroxyl concentrations between the first three oxides indicates that the inaccessibility to the surface sites may not be the major reason for the non-adsorption of the PEO.

### Heat of Wetting of Oxides

The enthalpy of interaction of water molecules with the surface hydroxyls is measured as the heat of wetting of the oxides (see Table 5.2)[Che59;Hea65]. It is observed that the heat of wetting of oxides follow the same trend as the concentration of surface hydroxyls. However, the interaction of water per surface hydroxyl show a considerable overlap for the oxides under consideration. This indicates that the water molecules are bonded with a similar strength to the surface hydroxyls on any oxide. The nature of surface hydroxyls, however, on different oxides may not be the same and this aspect is discussed next.

### Nature of Surface Hydroxyls

#### Point of Zero Charge of Oxides

For oxides with a hydrated surface, the surface chemistry in water is dominated by the chemical reactions

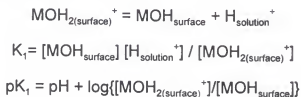


Table 5.2. Heat of Wetting values for oxides in water [Che59; Hea65].

Solid	Heat of wetting (ergs/cm <sup>2</sup> )
Quartz	260-370
Amorphous silica	165-220
Rutile (TiO <sub>2</sub> )	550, 550
Fe <sub>2</sub> O <sub>3</sub>	530
Al <sub>2</sub> O <sub>3</sub>	650-900

$$\begin{aligned}\text{MOH}_{\text{surface}} &= \text{MO}^{-1}_{\text{surface}} + \text{H}^{+}_{\text{solution}} \\ K_2 &= [\text{MO}^{-1}_{\text{surface}}] [\text{H}^{+}_{\text{solution}}] / [\text{MOH}_{\text{surface}}] \\ \text{p}K_2 &= \text{pH} + \log\{[\text{MOH}_{\text{surface}}] / [\text{MO}^{-1}_{\text{surface}}]\}\end{aligned}$$

where M represents a metal ion at the surface.

From these relations the point of zero charge (PZC) of the surface may be defined in terms of the pK's of reactions, i.e.,

$$\text{PZC} = 0.5 [\text{p}K_1 + \text{p}K_2]$$

and indicates the average acid-base characteristic of the surface. At any given pH, if an oxide surface donates relatively more protons than other it is more acidic and hence will have a lower pzc. In other words, the point of zero charge of an oxide is directly related to the acidity of the surface hydroxyl groups. The acidic surface hydroxyls are referred to as Bronsted acid sites (see Figure 5.1).

#### Correlation between Heat of Wetting and pzc of Oxides

Healy and Fuerstenau [Hea65] showed a linear correlation between the heat of wetting of oxides in water and their pzc (see Figure 5.2). This substantiates the assumption made in the preceding section that although the nature of the surface hydroxyls varies on different oxides the interaction strength with water molecules per surface hydroxyl is similar. Thus the role of solvent is not expected to be significantly different in PEO adsorption on the various oxides in aqueous medium.

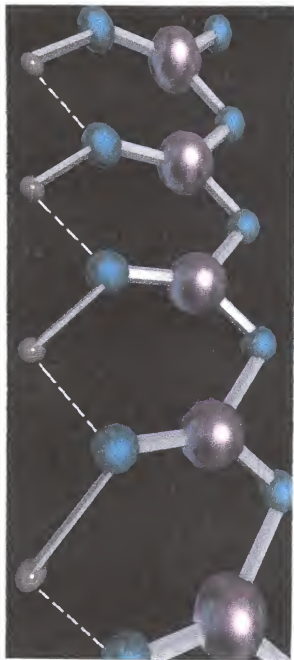


Figure 5.1. Schematic showing Bronsted acid sites.  
Purple = cation  
Blue = oxygen atoms.  
Grey = hydrogen atoms.

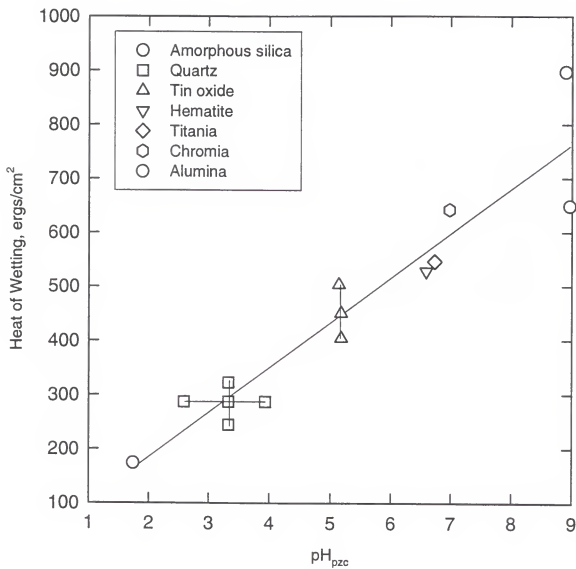


Figure 5.2. Heat of wetting of oxides as a function of their point of zero charge (after [Hea65]).

### Role of Bronsted Acidity in PEO Adsorption

#### Strength of Bronsted Acid Site and Electronegativity of Cation

It is shown above that the acidity of the Bronsted sites is the strongest on silica and the weakest on magnesia among the oxides under consideration. This can be understood qualitatively in terms of the electronegativity of the metal ion to which the surface hydroxyls are attached. The electronegativity of the surface metal atom governs the extent to which the electron pair shared between the metal and oxygen atoms is displaced towards the oxygen end.

In case of a predominantly ionic bond such as in MgO the electron pair is close to the oxygen atom which results in a stronger attraction for the proton. Frequency shifts in the IR spectra observed during water and benzene adsorption on MgO indicated that these hydroxyl groups are more basic than those on silica surface [And65]. However, for an oxide with a significant character of covalent bond e.g. SiO<sub>2</sub> the proton will not be strongly bound to the oxygen and therefore this type of hydroxyl is expected to be acidic. Al<sub>2</sub>O<sub>3</sub> has a more covalent character of Al-O bond than Mg-O but at the same time it is more ionic compared to SiO<sub>2</sub>. Thus, acidity of Bronsted sites is stronger on silica than on alumina.

The dependence of electronegativity on the type of bonding and electronic environment was shown by Pauling [Pau63]. This implies that strict comparisons between oxides as regards to their surface acidity should be made only for a particular type. Thus for MO<sub>2</sub> type of oxide the pzc should increase in the order



because the electronegativity differences increase from 1.7 for silica to 2.0 for zirconia. The higher acidity of Bronsted sites on silica than titania thus explains the

adsorption behavior of PEO for the two oxides. This also illustrates the sensitivity of the interaction of the ether oxygen of PEO to the acid strength of the Bronsted sites.

#### Relation Between Type of Oxide and its Point Of Zero Charge

Parks [Par65] has summarized the broad probable ranges of the pzc characteristic of the cation oxidation state from the known literature values which are reproduced in Table 5.3. The relation between the pzc and the cationic size and charge was explained by an electrostatic model involving the coordination number with crystal field and hydration corrections. It is noted that the isoelectric points determined for the oxides under consideration are in close agreement with the predicted values given in Table 5.3.

It is predicted from Table 5.3 that  $\text{MO}_3$  and  $\text{M}_2\text{O}_5$  type of oxides should exhibit stronger Bronsted acidity than the other oxide types. The validation of Parks model [Par65] has been corroborated for  $\text{MoO}_3$  and  $\text{V}_2\text{O}_5$  by spectroscopic investigations using probe molecules of known acidity or basicity.

It has been established through infra-red studies of adsorbed probe molecules that proton acid centers in simple oxides are essentially different in strength [Hai67;Dav90]. For instance, pyridine, a molecule only slightly less basic than ammonia, is not protonated on the surface of alumina which indicates that alumina has weak proton-donating properties [Cha63]. On the other hand,  $\text{MO}_3$  and  $\text{M}_2\text{O}_5$  type of oxides such as  $\text{MoO}_3$  and  $\text{V}_2\text{O}_5$  respectively protonate not only pyridine but such weak bases as propene and ethene [Dav90]. Experimental data indicate

Table 5.3. Probable ranges of pzc of different types of oxides [Par65].

Oxide	$M_2O$	$MO$	$M_2O_3$	$MO_2$	$MO_3, M_2O_5$
pzc, pH	>11.5	8.5 -12.5	6.5 -10.4	0 - 7.5	< 0.5

that the strongest Bronsted centers may be associated with the presence of  $\text{Mo}^{6+}$  ions. Thus oxides such as  $\text{MoO}_3$  and  $\text{V}_2\text{O}_5$  are expected to exhibit stronger Bronsted acid sites than silica and should adsorb and flocculate with PEO.

#### Adsorption and Flocculation Behavior of $\text{MoO}_3$ and $\text{V}_2\text{O}_5$ with PEO

Assuming that it is the presence of Bronsted acid sites with a strength comparable to or more than the acidic hydroxyls on surface of silica which is required to facilitate adsorption of PEO,  $\text{MoO}_3$  and  $\text{V}_2\text{O}_5$  should exhibit adsorption of PEO and flocculate.

#### Electrokinetic studies

It is observed from the electrokinetic behavior of  $\text{MoO}_3$  and  $\text{V}_2\text{O}_5$  shown in Figure 5.3 that both the materials exhibit high negative zeta potentials in the pH range studied. According to the prediction of pzc in Table 6.2, both the oxides have a pzc of less than pH 2.0. The electrokinetic studies on  $\text{MoO}_3$  and  $\text{V}_2\text{O}_5$  are also in agreement with the reported pzc values of 0.5 and 1.5 respectively [Par65]. The suspensions for both the samples drifted back to the natural pH of about 2.7 within an hour of measuring the zeta potentials. Thus, adsorption and flocculation tests with these oxides were attempted only at pH 3.0.

#### Adsorption of PEO on $\text{MoO}_3$ and $\text{V}_2\text{O}_5$

Adsorption isotherms for both  $\text{MoO}_3$  and  $\text{V}_2\text{O}_5$  with PEO of MW = 5,000,000 are shown in Figure 5.4. Both the isotherms are of high affinity type similar to that for silica (see Figures 4.10 and 4.11). The saturation adsorption densities of all the oxides as a function of their acidic strength, which is measured by the pzc, are summarized in Figure 5.5. The saturation adsorption densities of PEO on all the

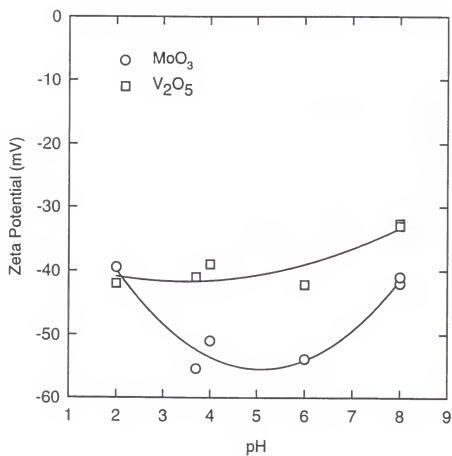


Figure 5.3. Electrokinetic behavior of  $\text{MoO}_3$  and  $\text{V}_2\text{O}_5$  suspensions as function of pH.

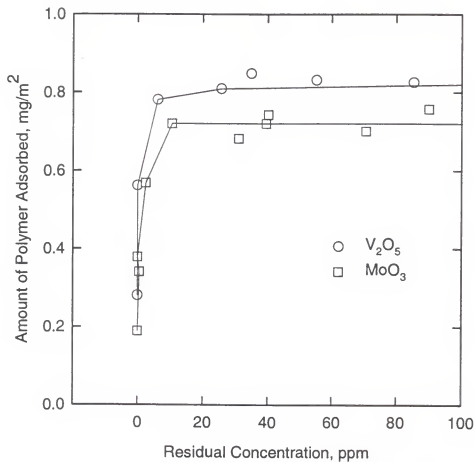


Figure 5.4. Adsorption isotherms of PEO on  $\text{MoO}_3$  and  $\text{V}_2\text{O}_5$  suspensions (PEO MW = 5,000,000; pH 3.0).

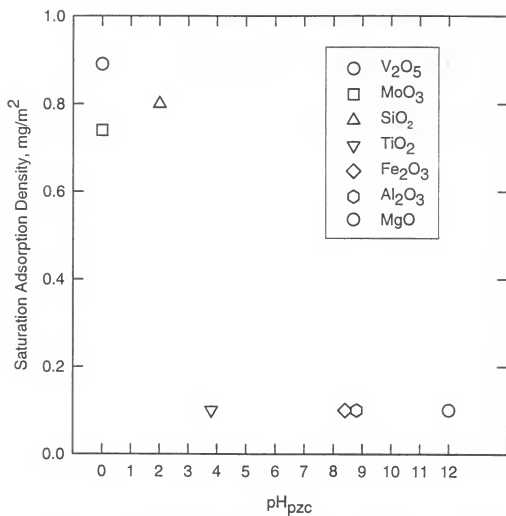


Figure 5.5. Saturation adsorption density of PEO (MW = 5,000,000) at pH 3.0 as a function of the point of zero charge of the oxides.

three oxides are similar indicating a similar adsorption mechanism. The insignificant adsorption of PEO on  $\text{TiO}_2$  indicates the sensitivity of the interaction of the ether oxygen with the surface Bronsted acid sites. Only those  $\text{MO}_2$  type oxides with a pzc lesser than that of silica are expected to adsorb PEO.

#### Flocculation behavior of $\text{MoO}_3$ and $\text{V}_2\text{O}_5$ with PEO

The flocculation behavior of  $\text{MoO}_3$  and  $\text{V}_2\text{O}_5$  as a function of the molecular weight of PEO is plotted in Figure 5.6. It is observed that for both the oxides the critical molecular weight for flocculation is 5,000,000 PEO. Large flocs which were retained over 400 mesh screen, as in the case of silica, were formed. This, to our knowledge, is the first report of flocculation of any oxide other than silica with PEO.

The flocculation of the two oxides with PEO as a function of dosage is plotted in Figure 5.7. It is observed that the breadth of flocculation decreases with increase in the molecular weight of the flocculant. The breadth of flocculation is larger for  $\text{MoO}_3$  and  $\text{V}_2\text{O}_5$  than  $\text{SiO}_2$  with PEO of 8,000,000 MW (see Figures 4.2 and 5.7). Silica flocculation is reduced to 20% at 8 mg/g while the other two oxides flocculate to the extent of more than 60% at dosage of 15 mg/g. The critical molecular weight of PEO for flocculation of silica is 8,000,000 while that for  $\text{MoO}_3$  and  $\text{V}_2\text{O}_5$  is 5,000,000. It appears from these observations that the breadth of flocculation increases with the flocculant molecular weight greater than the critical value.

#### Surface charge and PEO adsorption

It was shown in Chapter 4 that a negatively charged surface repelling PEO molecules is not a valid mechanism to explain the decrease of PEO adsorption with increasing pH. Further evidence that the PEO adsorption is not affected by the

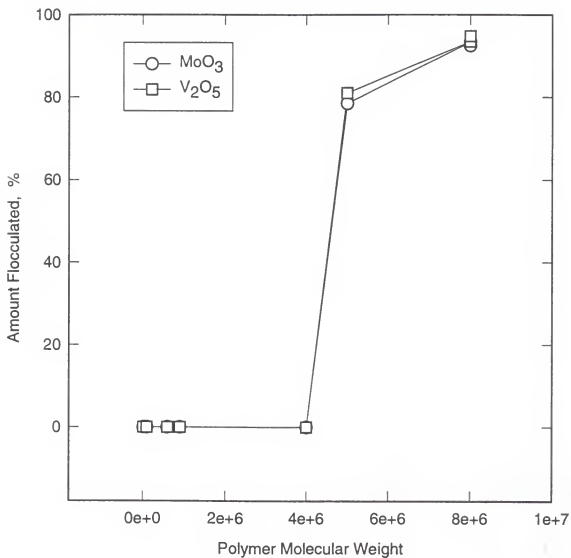


Figure 5.6. Flocculation behavior of MoO<sub>3</sub> and V<sub>2</sub>O<sub>5</sub> as a function of PEO molecular weight (dosage = 0.5 mg/g; pH = 3.0).

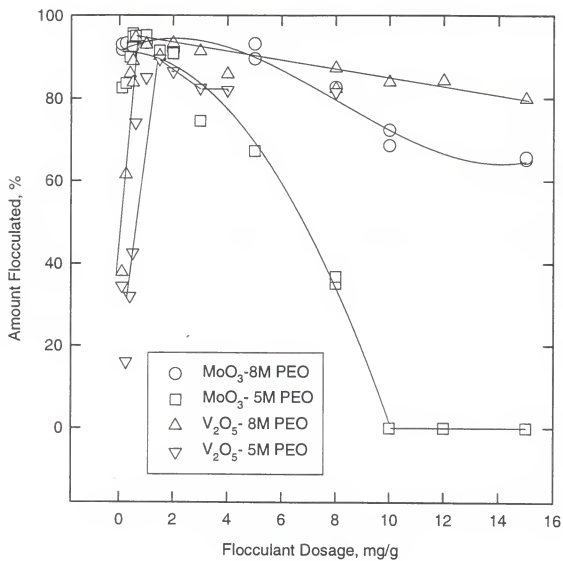


Figure 5.7. Flocculation of  $\text{MoO}_3$  and  $\text{V}_2\text{O}_5$  as a function of PEO dosage at pH 3.0.

negatively charged surface has been provided by adsorption and flocculation of  $\text{MoO}_3$  and  $\text{V}_2\text{O}_5$  with PEO at pH 3.0 ( $> -40$  mV zeta potential).

It was also shown in Chapter 4 that the presence of adsorbed ions, which in solution state are capable of complexing with the ether oxygen, does not significantly affect PEO adsorption. It is, however, possible that complexation of the dissolved ions from  $\text{MoO}_3$  and  $\text{V}_2\text{O}_5$  with ether oxygen may occur in solution and subsequent precipitation of the complex on the surface may lead to PEO adsorption. The complexation of Mo ions with PEO in aqueous solution was shown by Vassilev et al [Vas86]. Tests were therefore conducted to isolate the role of dissolved ions in the PEO adsorption process.

#### Effect of dissolved ions

Dissolution studies.  $\text{MoO}_3$  suspension was aged for 1 hour and the supernatant used to condition  $\text{Al}_2\text{O}_3$  and  $\text{TiO}_2$  powders to determine the adsorption of dissolved ions on the  $\text{Al}_2\text{O}_3$  and  $\text{TiO}_2$  surfaces respectively (see Table 6.4). It is observed that the maximum adsorption occurs on  $\text{Al}_2\text{O}_3$  while the least on  $\text{SiO}_2$ . This is expected since at pH 3.0  $\text{Al}_2\text{O}_3$  is positively charged while  $\text{SiO}_2$  is slightly negatively charged and the dissolved Mo is present as negatively charged species  $\text{MoO}_4^{2-}$  [Kun89]. The formation of crystalline  $\text{MoO}_3$  on the underlying substrate occurs only when more than 4.5 Molybdenum atoms/ $\text{nm}^2$  of the surface are present [Kun89]. In the present case, monomeric ions are expected on  $\text{SiO}_2$  ( $\leq 1$  Molybdenum/ $\text{nm}^2$ ) while heptameric species,  $\text{Mo}_7\text{O}_{24}^{6-}$ , and an octahedrally coordinated polymeric surface species are present on  $\text{Al}_2\text{O}_3$  and  $\text{TiO}_2$  (1-4.5 Molybdenum/ $\text{nm}^2$ ) [Oka88;Kun89].

Table 5.4. Dissolution behavior of  $\text{MoO}_3$  and  $\text{V}_2\text{O}_5$  powders and the adsorption of dissolved ions on other oxides.

pH = 3.0

Solids loading 2g/100 ml

Aging time = 3600 s

Amount of Molybdenum dissolved = 330.6 ppm (16.5 mg/g solids)

Amount of Vanadium dissolved = 275.1 ppm (13.7 mg/g solids)

Oxide	Residual in solution after 6h (ppm)	Amount of Molybdenum adsorbed ( $\text{mg/m}^2$ )	Number of Molybdenum ions per $\text{nm}^2$ of oxide surface
$\text{TiO}_2$	280.5	0.23	1.4
$\text{Al}_2\text{O}_3$	268.5	0.44	2.7
$\text{SiO}_2$	320.5	0.16	1.0

PEO adsorption and flocculation of Mo coated oxides. The non-flocculation behavior of the molybdenum coated alumina and titania was corroborated by adsorption studies wherein no measurable adsorption of 8,000,000 MW PEO was detected indicating that adsorbed ions do not cause adsorption of PEO. Thus it is shown that adsorbed ions do not cause adsorption of PEO. It is expected though that formation of crystalline  $\text{MoO}_3$  on the surface of a non-flocculating oxide may lead to PEO adsorption. In another study surface modification of  $\text{Al}_2\text{O}_3$  by surfactant coating was found to result in PEO adsorption [Ram88]. However, PEO adsorption occurred only after the initiation of hemi-micellization of the surfactant on the alumina surface [Ram88]. This may be due to the interaction between the induced hydrophobic sites on alumina through hemi-micelle formation and the hydrophobic  $(\text{CH}_2\text{-CH}_2)\text{-}$  moiety of the PEO. Thus surface chemical modification through formation of either crystalline  $\text{MoO}_3/\text{V}_2\text{O}_5$  or hemi-micelles of oxides not amenable to flocculation with PEO present alternative routes to induce PEO adsorption.

#### Role of Lewis Acid Sites

It has been shown so far that the adsorption of PEO on oxides is sensitive to the acidity of the surface Bronsted sites. The other type of acid sites present on the oxide surfaces are Lewis sites which are exposed cations with unsaturated valence as illustrated schematically in Figure 5.8. It is known that the strongest Lewis acid sites ( $\text{Al}^{3+}$  ions) are found on alumina surface [Dav90]. In principle, an acid-base interaction should be expected between the exposed  $\text{Al}^{3+}$  ions and ether oxygen of PEO. The  $\text{Al}^{3+}$  Lewis acid site on exposure to water does not convert to

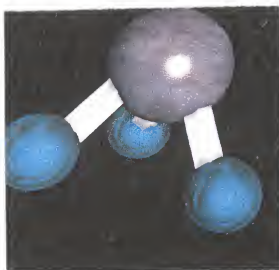


Figure 5.8. Schematic showing a Lewis acid site (exposed cation).  
Large sphere = exposed cation  
Small spheres = oxygen atoms.

a Bronsted site [Parr63] and thus there exists a possibility of  $\text{Al}^{3+}$  ion and ether oxygen interaction.

#### Oxide/PEO/ $\text{CCl}_4$ system

van der Beek [Van91] has shown that in  $\text{CCl}_4$  solvent the adsorption energies for various polymers are larger on silica than on alumina. The strength of the segment-surface interaction for different polymers varied in the same fashion for both alumina and silica. The adsorption energy of PEO was determined to be 1 kT higher on silica than on alumina and this was the largest energy difference between adsorption on silica and alumina for the polymers examined. This energy difference on silica and alumina may indicate that OH groups are more accessible for ether groups than Lewis acid sites. Ether groups in the main chain of adsorbate molecules are less exposed than functional end groups present on other polymers and are therefore more sterically hindered to acquire optimal orientations on the substrate. This steric hindrance will be more for Lewis acid sites than for hydroxyl groups because Lewis acid sites have more rigidly fixed positions on the surface than the protons taking part in hydrogen bonding. The hydroxyl groups have the ability to rotate and may therefore adjust their direction to the adsorbing groups for optimal interactions. Hence, the adsorption energy is significantly affected by steric hindrance between adsorbate molecules and Lewis acid sites compared to interaction between the ether groups and Bronsted acid sites.

#### Hematite/Starch/Water System

The interaction of Lewis acid sites with the adsorbate polymer molecules has recently been illustrated in the hematite-starch system [Pra91; Wei95]. Hydrogen

bonding between starch hydroxyl groups and mineral surface hydroxyl groups has been the favoured mechanism for many years mainly because of the presence of a large number of hydroxyl groups on the starch and mineral surfaces [Iwa82]. Later, evidence was obtained to suggest that a chemical interaction between the polysaccharide and the mineral is the likely mechanism for adsorption [Kho84]. Pradip postulated this interaction as a molecular recognition mechanism of Fe surface sites and the ether oxygen groups in starch molecule [Pra91]. Recently, Weissenhorn and co-workers [Wei95] have shown through DRIFT studies that Fe sites on the surface of hematite participate in interaction with amylopectin and that hydrogen bonding plays a minor role in starch adsorption.

An important conclusion from the hematite-starch system is that hydrogen bonding cannot be postulated as an interaction mechanism just because seemingly appropriate functional groups are present on the adsorbate and the adsorbent. It is the chemical nature of the surface sites that determines the bonding to the polymer functional groups. It must be noted that the functional groups in starch are not in the backbone chain like the ether oxygen in PEO and hence interaction with the Lewis acid sites is more probable for the former. The PEO molecule, however, also shows specificity of hydrogen bonding to oxide surfaces by interacting only with strong Bronsted sites as shown in the preceding sections.

## CHAPTER 6

### CHARACTERIZATION OF PEO BINDING SITES ON OXIDE SURFACES

#### Introduction

It is generally accepted that the hydroxyl coverage on oxide surfaces occurs as a result of water dissociation, assuming that every surface oxygen joins the hydrogen atom and the water OH groups are bound to metal atoms (see schematic in Fig 6.1). The evidence for chemical surface hydration of oxides has been provided by infrared absorption studies, heat of wetting measurements, and the thermal behavior of the adsorption-desorption kinetics of water. These studies have also shown that the surface hydroxyls on a given oxide are not equivalent in their chemical nature [You58;Hai67;Roc75].

It was observed that although silica A and silica B show similar affinity for PEO at pH 3.0, in Chapter 4, their behavior was significantly different at pH 9.5. Previous work on silica-PEO/PVA system identified the isolated silanols as the principal binding sites for the ether oxygen of PEO [Rub76;Che85;Kha87]. In this Chapter surface characterization of the silica samples as well as other oxides via DRIFT studies is described to further elucidate the role of isolated hydroxyls in PEO adsorption. Additionally, it was shown in Chapter 5 that the acidity of the surface hydroxyls on oxides determines the interaction with the ether oxygen of PEO. The surface acidity of the oxides is also characterized by DRIFT studies using pyridine as the probe molecule.

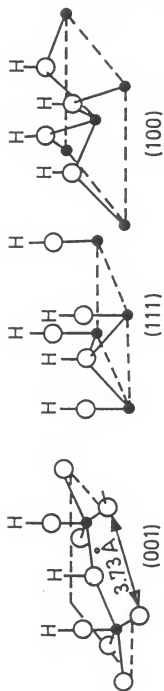


Figure 6.1. Schematic showing surface hydroxylation on various faces of anatase.

### Surface Hydroxyls on Oxides

The DRIFT spectra of the oxide samples in the hydroxyl region (3000–4000  $\text{cm}^{-1}$ ) are shown in Figures 6.2 and 6.3.

#### Silica A

The DRIFT spectra of silica A (see Figure 6.2) shows the presence of isolated hydroxyl groups as a shoulder at 3747  $\text{cm}^{-1}$ . An isolated silanol is not hydrogen bonded since the minimum O–H...O distance between neighboring silanols exceeds about 0.33 nm, equivalent to the normal van der Waals O...O contacts for non-bonded oxygen atoms. In accordance with Tsyganenko and Filimonov [Tsy72], only one type of isolated hydroxyl was observed on the silica surface. They demonstrated that the ultimate number of isolated hydroxyl groups possible on an oxide is one unit less than the oxygen coordination number which is two in the case of silica.

The hydrogen bonding interactions give rise to other types of hydroxyls on the silica surface. The vicinal silanols are hydroxyl groups located on neighboring sites such that they may hydrogen bond with one another. In Figure 6.2 these are characterized by the band at 3649  $\text{cm}^{-1}$ . The broad band at 3470  $\text{cm}^{-1}$  is due to the adsorption of molecular water. A similar spectra for the Stober silica was obtained by Cheng [Che85] and Khadilkar [Kha87].

#### Alumina-A

$\alpha$ -alumina is of corundum structure and has an oxygen coordination number of three. Thus, at the most, only two types of isolated hydroxyls can exist on the alumina surface which are observed at 3735 and 3700  $\text{cm}^{-1}$  (see Figure 6.2).

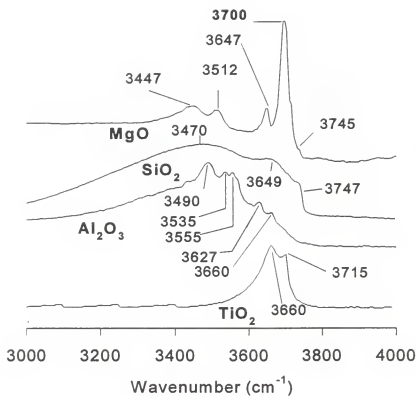


Figure 6.2. DRIFT spectra of oxides in the hydroxyl region.

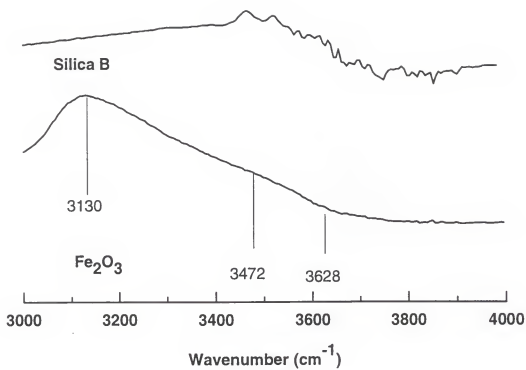


Figure 6.3 DRIFT spectra of silica B and hematite in the hydroxyl region.

Several bands due to hydrogen bonded hydroxyls in the range  $3660-3500\text{ cm}^{-1}$  were also observed. The presence of molecular water on the alumina surface is indicated by the band at  $3490\text{ cm}^{-1}$ . The characterization of the surface hydroxyls on  $\alpha$ -alumina is in agreement with that of Morterra et al [Mor76].

### Magnesia

Magnesia has the NaCl structure where oxygen atoms are octahedrally surrounded by six metal atoms. In principle, five types of hydroxyls are possible for such a lattice and their presence is dependent upon the number of M-O bonds (1, 2 or 3 respectively) intersected by the cleavage plane. The bands attributed to isolated hydroxyls, as shown in Figure 6.2, occur at  $3745$ ,  $3700$  and  $3647\text{ cm}^{-1}$ . Anderson et al [And65b] reported the presence of isolated hydroxyls at  $3750$  and  $3630\text{ cm}^{-1}$  for a MgO crystal where the cube face (100) was predominant. The band at  $3512\text{ cm}^{-1}$  can be ascribed to mutually bonded hydroxyls while that at  $3447\text{ cm}^{-1}$  is due to the presence of molecular water. At this stage it is important to note that the isolated hydroxyl groups for magnesia occur at a similar wavenumber as on silica. However, shifts observed during water and benzene adsorption on magnesia indicate that these hydroxyl groups are more basic than on silica [And65b].

### Titania

The anatase form of titania showed two bands at  $3715$  and  $3660\text{ cm}^{-1}$  which are due to isolated and bonded hydroxyls respectively (see Figure 6.2). These band assignments are in accordance with the previous work of Primet et al [Pri71].

### MoO<sub>3</sub> and V<sub>2</sub>O<sub>5</sub>

The DRIFT spectra of MoO<sub>3</sub> and V<sub>2</sub>O<sub>5</sub>, as illustrated in Figure 6.2, is relatively featureless in the 3400-3800 cm<sup>-1</sup> region. This behavior has been attributed to the high mobility of the proton on the surface of these oxides [Dav90].

### Hematite

The DRIFT spectra of hematite presented in Figure 6.3 showed a broad band at 3130 cm<sup>-1</sup> due to adsorption of molecular water on the surface. The band positions of the isolated and hydrogen bonded hydroxyls are also indicated on the spectra [Hai67].

### Silica B

The surface of silica B shows the presence of hydrogen bonded hydroxyls and molecularly bonded water while the characteristic band of amorphous silica at 3747 cm<sup>-1</sup> is not observed (see Figure 6.3). This may be due to the crystallinity of silica B which apparently presents a different surface structure than silica A which is completely amorphous.

### Isolated Hydroxyls and PEO Adsorption

The band positions of the various types of hydroxyls along with the saturation adsorption density of 5,000,000 MW PEO are summarized in Table 6.1. The absence of isolated hydroxyls on silica B, MoO<sub>3</sub> and V<sub>2</sub>O<sub>5</sub> along with the presence of isolated hydroxyls on non-adsorbing oxides indicates that there is no correlation between the presence of isolated hydroxyls and adsorption of PEO. However, such a correlation may exist for isolated silanols and PEO adsorption [Che85].

Table 6.1. Surface hydroxyls on different oxides and the saturation adsorption density of PEO.

Oxide	Hydroxyls		Adsorption Density <sup>☆</sup> , mg/m <sup>2</sup>
	Isolated	Bonded	
MoO <sub>3</sub>	Not observed due to high mobility of proton.		0.73
V <sub>2</sub> O <sub>5</sub>			0.84
SiO <sub>2</sub> (A)	3747	3649 3470	0.80
SiO <sub>2</sub> (B)		3470	0.63
TiO <sub>2</sub>	3715	3660	< 0.1
Al <sub>2</sub> O <sub>3</sub>	3735 3700	3660 3627 3555 3535 3490	
Fe <sub>2</sub> O <sub>3</sub>	3628	3472 3130	
MgO	3745 3700 3647	3512 3447	

☆ Saturation adsorption density, measured at pH 3.0 with 5,000,000 MW PEO.

Rubio and Kitchener [Rub76] and Cheng [Che85] suggested isolated silanols to be the primary binding sites for PEO adsorption on the basis of changes in adsorption and the concentration of the isolated silanols with heat pretreatment. Upon heat treatment, the molecular water and hydrogen bonded hydroxyls are driven off the surface leading to an increase in the relative concentration of the isolated silanols. Thus heat treatment studies, therefore, were carried out for both types of silica samples to further elucidate the role of isolated silanols in the adsorption of PEO. Also, the accessibility of the surface sites to the PEO molecules was investigated by dehydroxylating the surface of alumina through heat pretreatment.

#### Effect of Heat Pretreatment

##### Silica

A comparison of the DRIFT spectra for heat treated silica A with the untreated sample in Figure 6.4 reveals that the isolated hydroxyl peak for silica A sharpens with temperature and at 1100°C only isolated silanols are present.

The surface of silica B when heat treated to 800°C reveals an essentially dehydroxylated surface. The different speciation of OH groups on silica B may be attributed to its crystalline nature which presents a different surface structure than the amorphous silica A [Ile79]. The speciation of OH groups on amorphous silica surface has been shown to depend on the siloxane ring size, degree of ring opening, number of OH per surface silicon site [Bri90] and also surface curvature [Ile79] (see Figure 6.5). The convex surface, as of spherical silica A particle, may cause the neighboring OH to be isolated in nature (see Figure 6.5).

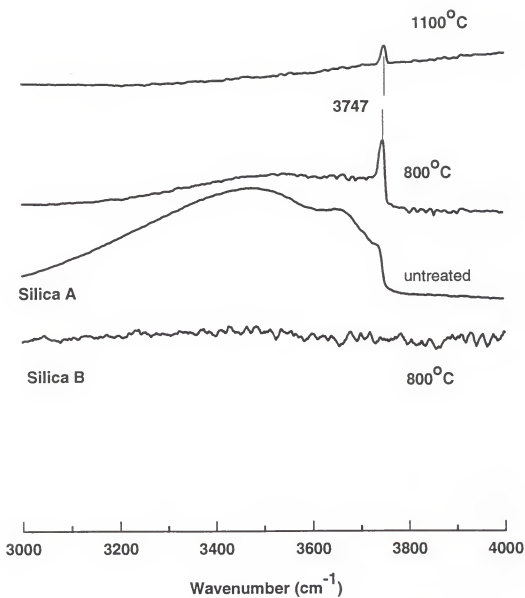
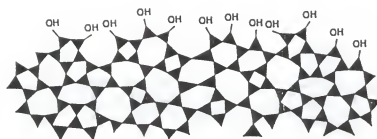
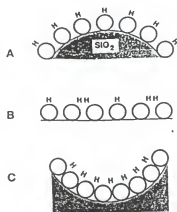


Figure 6.4. DRIFT spectra of heat treated silica samples.



(i)



(ii)

Figure 6.5. Schematic of i) amorphous silica surface showing the ring structure and ii) influence of surface curvature on H-bonding. A. Small positive radius of curvature reduces H-bonding between neighboring silanols. B. Large radius of curvature facilitates more hydrogen bonds. C. Negative radius of curvature exhibits strongest H-bonding.

### Alumina-A

In the case of alumina, heat treatment at 800°C resulted in the prominence of the bands corresponding to the isolated hydroxyl groups at 3735 and 3700  $\text{cm}^{-1}$  (see Figure 6.6). The hydrogen bonded hydroxyls decreased and are not clearly resolved in the IR spectra. The band attributed to molecular water at 3490  $\text{cm}^{-1}$  (see also Figure 6.2) shifts to lower wavenumber of about 3350  $\text{cm}^{-1}$ . At 1100°C, the intensities of all these bands are significantly reduced. A similar evolution of IR spectra with heat treatment on Alumina A was earlier reported by Dow [Dow92].

### Adsorption of PEO on Heat Treated Samples

#### Silica

It is seen from Figure 6.7 that silica A, which exhibits only isolated silanols at 1100°C, adsorbs PEO confirming that isolated silanols are indeed the principal binding sites for PEO adsorption. The adsorption density of the heat treated surface (0.45  $\text{mg/m}^2$ ), however, was slightly lower than the untreated sample of silica A (0.62  $\text{mg/m}^2$ ). This follows the trend of saturation adsorption density of PEO and the concentration of isolated silanols on silica upon heat pretreatment [Che85].

Rubio and Kitchener [Rub76] postulated that the isolated hydroxyls on the silica samples disappeared when heated over 1000°C which led to insignificant adsorption of PEO. The existence of isolated silanols at 1100°C and the adsorption of PEO on silica A, pretreated to 1100°C, appears to be in contradiction to their observations. This apparent discrepancy may probably due to the synthesis conditions along with high surface area (greater than 50  $\text{m}^2/\text{g}$ ) of the silica samples used in their study. In the present investigation the silica A has a surface area of

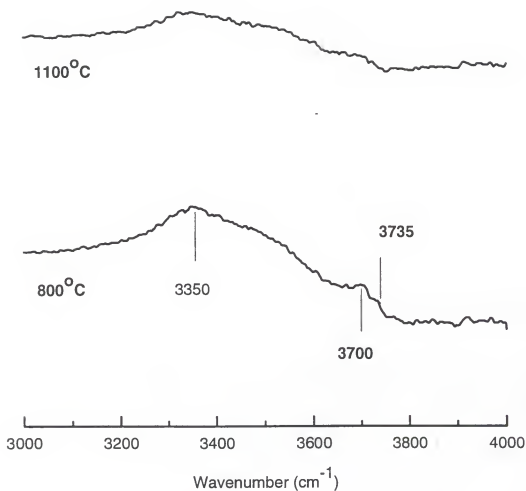


Figure 6.6. DRIFT spectra showing the effect of heat treatment on the surface hydroxylation of alumina A.

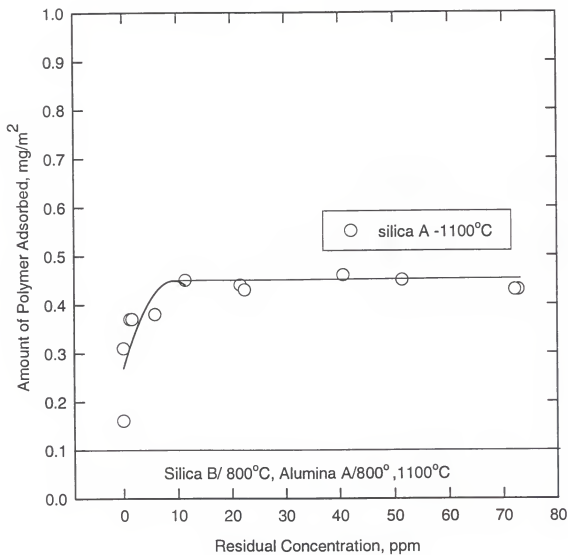


Figure 6.7. Adsorption isotherms of PEO for heat-treated oxides at pH 9.5 (PEO MW = 5,000,000).

about  $3.2 \text{ m}^2/\text{g}$ . The viscous sintering, therefore, could have initiated at a lower temperature for high surface areas silica thereby leading to annihilation of the isolated silanols at lower temperatures.

The absence of hydroxyls on silica B in the DRIFT spectra was reflected in the loss of adsorption of PEO compared to the untreated sample (see Figure 4.10). The lack of PEO adsorption on a dehydroxylated silica surface has been attributed to a hydrophobic surface consisting of essentially siloxane groups [Rub76].

### Alumina

Heat treatment of Alumina A did not seem to change the low PEO saturation adsorption density as shown in Figure 6.7. The lack of adsorption of PEO on alumina irrespective of pH and heat pretreatment thus indicates that the surface hydroxyls are not acid enough to interact with the ether oxygen. Robinson et al [Rob64] found that the isoelectric point of alumina decreased to about 6.7 from 9.0 upon calcination of the sample at  $1400^\circ\text{C}$ . Thus heat pretreatment alone does not appear to induce sufficient acidity of surface hydroxyls to facilitate interaction with the ether oxygen of PEO.

The calcination of alumina leads to a progressively dehydroxylated surface which should mitigate the inaccessibility of the PEO molecules to the Lewis acid sites. Simultaneously, partial dehydroxylation is expected to result in an increase in the concentration of the Lewis acid sites. However, the absence of adsorption of PEO on partially dehydroxylated alumina further supports the concept that the strength of the Bronsted acid sites determines the binding of the ether oxygen of PEO.

### Characterization of Surface Acidity of Oxides

A measure of the strength of Bronsted acid sites is the point of zero charge of the oxide, as discussed in Chapter 05. Additionally, the surface acidity can be characterized by adsorption of probe molecules of known basicity. The pyridine molecule ( $K_b=10^{-4}$ ) is a weaker Lewis base than ammonia ( $K_b=10^{-3}$ ) and is therefore more sensitive to the type of acid site [Par63]. The various possible complexes that form upon adsorption and the corresponding frequencies are shown in Table 6.2.

#### DRIFT Spectra of Adsorbed Pyridine on Oxides

Pyridine adsorption shown in Figure 6.8 revealed that  $\text{MoO}_3$  and  $\text{V}_2\text{O}_5$  exhibit sharp peaks corresponding to the formation of pyridinium ions at 1485 and 1535  $\text{cm}^{-1}$  characteristics of the presence of strong Bronsted acid sites in agreement with previous studies [Dav90]. Silica A shows the presence of hydrogen bonded pyridine (bands at 1445 and 1595  $\text{cm}^{-1}$ ) indicating that the Bronsted acid sites are weaker than those present on  $\text{MoO}_3$  and  $\text{V}_2\text{O}_5$ . However, silica B, alumina A, magnesia, titania and hematite did not exhibit pyridine adsorption. The presence of stronger hydrogen bonding sites on silica A than alumina A indicated by pyridine adsorption is in agreement with the results of Parry [Par63]. It was determined that isolated silanols hydrogen bond with the pyridine molecules and can be removed by evacuation at 150°C [Par63]. On the other hand, hydrogen-bonded pyridine is removed from the alumina surface by evacuation at 25°C [Roc76]. The presence of weak Bronsted acid sites on alumina, magnesia, titania and hematite

Table 6.2 Infrared bands of pyridine in the 1400-1700  $\text{cm}^{-1}$  region of the spectrum. Band intensities are vs = very strong; s=strong; v=variable.

Hydrogen Bonded Pyridine	Coordinatively Bonded Pyridine	Pyridinium Ion
1440-1447 (vs)	1447-1460 (vs)	1485-1500 (vs)
1485-1490 (w)	1488-1503 (v)	1540 (s)
1580-1600 (s)	1580 (v)	1620 (s)
	1600-1633 (v)	1640 (s)

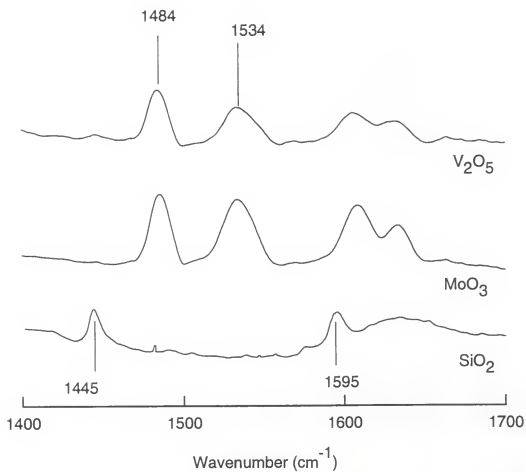


Figure 6.8. DRIFT spectra of pyridine treated  $\text{MoO}_3$ ,  $\text{V}_2\text{O}_5$  and  $\text{SiO}_2$  samples.

incapable of hydrogen bonding with pyridine, is in agreement with the characterization of surface acidity by point of zero charge of oxides.

#### Acidity of silanol groups

The absence of hydrogen bonding with pyridine for silica B is in contrast to silica A and may be due to a significantly lower concentration of strong Bronsted acid capable of bonding with pyridine. Model studies on silsequioxanes have revealed that sites of differing reactivity may be present depending on the extent of hydrogen bonding between the neighboring hydroxyls on the silica surface [Feh89;Feh90]. Isolated silanols were predicted to be less acidic than clusters possessing at least three mutually hydrogen bonded hydroxyl groups. This was experimentally shown to be the case by the calorimetric adsorption results of Chronister and Drago [Chr93]. These authors elucidated three hydrogen-bonding sites of different strengths with the isolated silanols being the weakest acidic site on the surface.

#### Surface Analysis of Silica and Adsorption of PEO

##### Specificity of hydrogen-bonding of isolated silanols

The isolated silanol sites, although not the most acidic, are still the stable sites for PEO adsorption as illustrated by the relative insensitivity of the adsorption isotherms for silica A to pH (see Figures 4.9 and 4.10). This stability may be due to their large concentration on the silica A surface which is exemplified by a significant adsorption of PEO on silica sample pretreated to 1100°C (see Figure 6.7). As a result of this pretreatment the isolated silanols were the only adsorption sites available on the silica surface.

In accordance with the results of Cheng [Che85] and Behl and Moudgil [Beh93d], no shift in the frequency of the isolated silanol groups on PEO coated silica A surface was noticed to indicate the specificity of the hydrogen bonding. This has been attributed to the presence of water molecules [Che85;Beh93d]. The effect of water molecules on the sensitivity of the measurements can be obviated by the use of non-aqueous solvents. In non-aqueous solvents direct evidence for hydrogen bonding of the isolated silanols to a copolymer of ethylene oxide-methyl methacrylate was obtained where large shift (about  $100\text{ cm}^{-1}$ ) was observed for the polymer coated silica particles [Fri62;How70].

The specific nature of the hydrogen bonding interactions of the isolated silanols with several organic molecules in vapor state including diethyl ether (the monomer group of PEO) was established by Kiselev [Kis65]. He determined that the specific heat of adsorption on the hydroxyl group,  $Q_a$  is approximately linearly related to the frequency shifts  $\nu_{OH}$  obtained upon adsorption of these molecules. This relationship is reproduced in Figure 6.9 [Kis65]. Basila [Bas61] proposed that since the heat of adsorption is inversely proportional to the ionization potential of the adsorbate, this relationship serves as evidence that the interaction between the hydroxyl groups and the adsorbate is essentially one of charge transfer. It is observed that the ether oxygen produced a larger shift ( $450\text{ cm}^{-1}$ ) than water ( $200\text{ cm}^{-1}$ ) indicating a stronger hydrogen bonding of the isolated silanols to the former [And65a;Kis65].

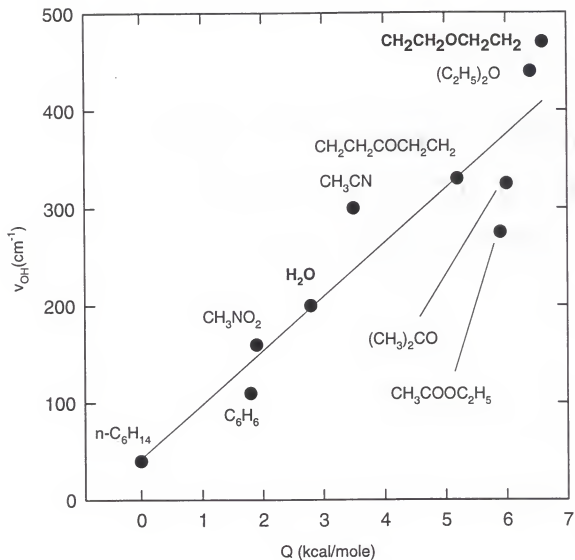


Figure 6.9. Plot of the change in frequency of isolated silanols against the specific heat of adsorption for several vapors adsorbed on silica surface (data after Kieslev [Kis65] and Anderson [And65a]).

### Effect of pH

The adsorption of PEO at pH 3.0 on silica B (see Figure 4.10) and the absence of isolated silanols indicate that other types of silanols with sufficient acidity to hydrogen bond with the ether oxygen of PEO must be present on the surface. However, at pH 9.5 a significantly lower PEO adsorption was determined on silica B and the silica plate. This suggests that with increasing pH the concentration of the binding silanol sites is considerably reduced. These silanols interact with the ether oxygen close to the isoelectric point, where they are present in the unionized form. Their ionization to a negatively charged surface species with increasing pH results in the loss of binding to the ether oxygen of PEO and a corresponding loss in PEO adsorption.

The presence of hydrogen bonded silanols on the silica surface, which are more acidic than the isolated silanols, has been predicted and experimentally validated, as discussed in the preceding section [Feh89;Feh90;Chr93]. Their dissociation will precede that of the isolated silanols on account of their higher acidity. The lower acidity of the isolated silanols along with their large concentration, estimated at about one-third of the total surface silanols [Arm69], may then be responsible for the relative insensitivity of PEO adsorption on silica A to pH changes.

## CHAPTER 7

### ADSORPTION AND FLOCCULATION BEHAVIOR OF SILICATES WITH PEO

#### Introduction

The silicate minerals essentially comprise of  $\text{SiO}_4$  tetrahedra and oxygen or hydroxyls octahedra containing divalent or trivalent cations. The different type of silicate structures, as discussed in Chapter 3, are essentially classified by the connectivity of the  $\text{SiO}_4$  tetrahedra. Thus the building blocks of silica and other oxides are present in the silicates.

The adsorption of PEO on silica and its flocculation behavior has been discussed in the rest of this study. The other simple oxides with a pzc greater than that of silica did not exhibit adsorption of PEO. Thus it is of interest to examine the adsorption behavior of PEO on mixed oxides containing silica and other oxides in the context of the PEO adsorption mechanism determined for oxides. In this Chapter the adsorption behavior of PEO on representative samples of each silicate type is discussed and the adsorption mechanism of PEO correlated with their structural characteristics.

#### Adsorption and Flocculation Studies

##### Flocculation of silicates

The flocculation behavior of the silicate samples as a function of the molecular weight of PEO is shown in Figure 7.1. It is observed that only layered

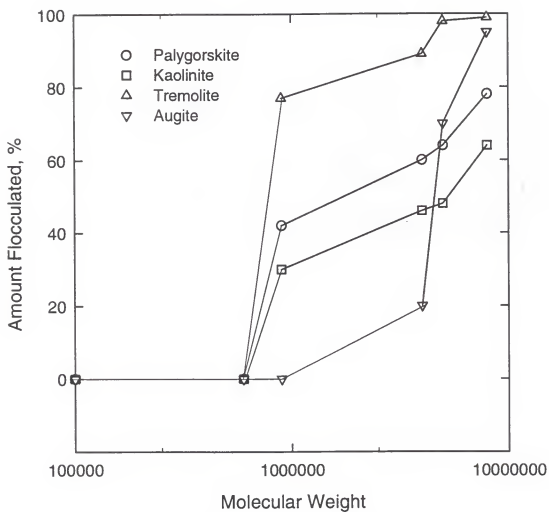


Figure 7.1. Flocculation of silicate samples as a function of molecular weight of PEO (pH = 9.5; dosage = 1mg/g)

(kaolinite and palygorskite) and chain (augite and tremolite) silicates flocculate while the orthosilicate minerals (almandine, olivine and topaz) do not. The critical molecular weight of PEO for flocculation of the silicate samples is summarized in Table 7.1. It is seen that for the clays and tremolite the critical molecular weight is 900,000 while for augite it is 4,000,000. It is well known that palygorskite, a predominant component of phosphatic clays, flocculates easily with PEO [Sch86;Bro89]. Similarly the flocculation of kaolinite with PEO was shown by Koksall et al [Kok90]. The flocculation behavior of pyroxene and amphibole type of silicates has been reported in the literature. The flocculation behavior of these two silicate minerals, therefore, is examined in detail in the following section.

#### Effect of Flocculant Dosage

##### Augite

It is observed that the flocculation of augite is independent of the dosage of PEO of 8,000,000 MW whereas a maximum in flocculation at a dosage of 0.5 mg/g is seen with PEO of 5,000,000 MW (see Figure 7.2). In fact, the flocculation behavior of augite with PEO is similar to that of  $\text{MoO}_3$  (see Figure 5.7). The optimum dosage of 5,000,000 and 8,000,000 MW PEO is similar for both the materials, being about 0.5 mg/g and 0.1 mg/g respectively. This implies that the number of molecules of 8000,000 MW PEO adsorbed per particle at the optimum dosage is nearly an order of magnitude lower than that for 5,000,000 MW PEO. This indicates that bigger polymer molecules form more or stronger bridges due to more segments in contact with the particle surface, although no quantitative explanation for this effect has been proposed yet. A similar result was obtained for

Table 7.1. Critical molecular weight for flocculation of the silicate minerals at pH 9.5.

Material	Critical Molecular Weight of PEO
Palygorskite	900,000
Kaolinite	900,000
Tremolite	900,000
Augite	4,000,000
Almandite	No flocculation
Olivine	
Topaz	

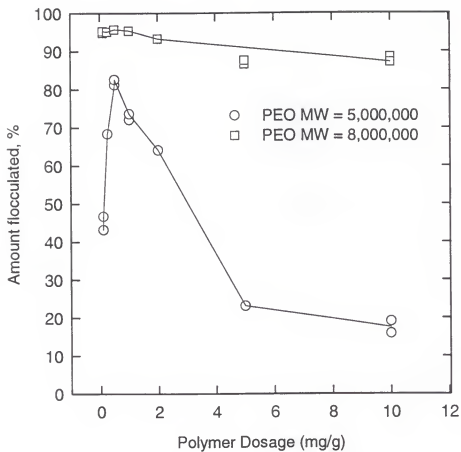


Figure 7.2. Flocculation behavior of augite as a function of PEO dosage at pH 9.5.

the latex-PEO system by Perssels et al [Per90]. As a result of fewer number of molecules of higher molecular weight polymer required for flocculation it may be possible that the flocculation rate is enhanced with respect to the adsorption kinetics. In such a case, prior to complete coverage of the surface by polymer molecules at higher dosages, stable flocs may already have been formed. This may, thus, explain the relative insensitivity of flocculation of augite and  $\text{MoO}_3$  to the dosage of PEO of 8,000,000 MW.

#### Tremolite

The flocculation of tremolite as a function of PEO dosage is plotted in Figure 7.4. It is observed that, similar to augite, the flocculation of tremolite is relatively insensitive to the polymer dosage for PEO molecular weight greater than the critical MW of 900,000.

#### Adsorption Studies on Silicates

The adsorption kinetics of PEO of 5,000,000 MW at a dosage 10 mg/g on tremolite and augite at pH 9.5 is presented in Figure 7.5. It is observed that after about 12 hours the adsorption reaches an equilibrium value for both tremolite and augite. An equilibration time of 16 hours, however, was used for deriving adsorption isotherms of PEO on the silicate minerals.

The adsorption isotherms of PEO on tremolite, augite, almandite, olivine and topaz at pH 9.5 are plotted in Figure 7.6. The adsorption isotherms for the layered silicates, kaolinite and palygorskite are presented in Figure 7.7. It is observed that the orthosilicates exhibit much lower adsorption compared to the layered and chain silicates. Thus the equilibrium time of 16 hours for the orthosilicates is justified on

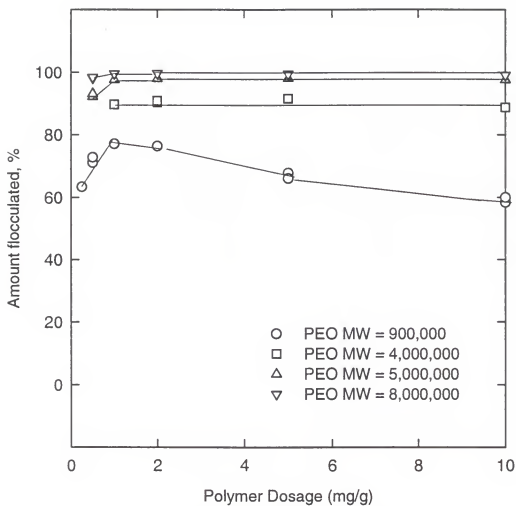


Figure 7.3. Flocculation behavior of tremolite as a function of PEO dosage at pH 9.5.

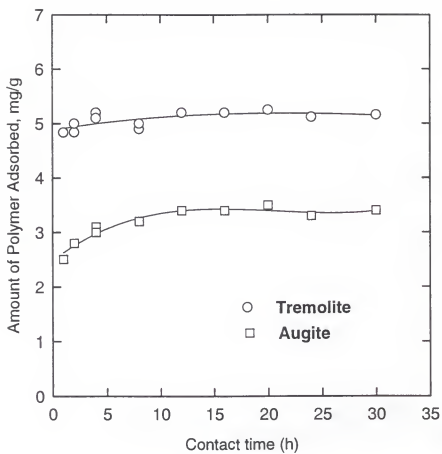


Figure 7.4. Kinetics of PEO adsorption on tremolite and augite.

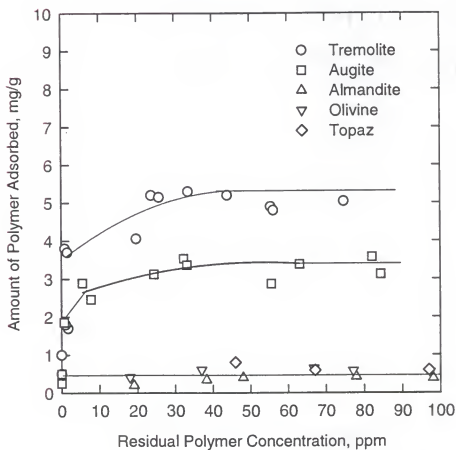


Figure 7.5. Adsorption isotherms of PEO on chain and orthosilicates at pH 9.5 (PEO MW = 5,000,000)

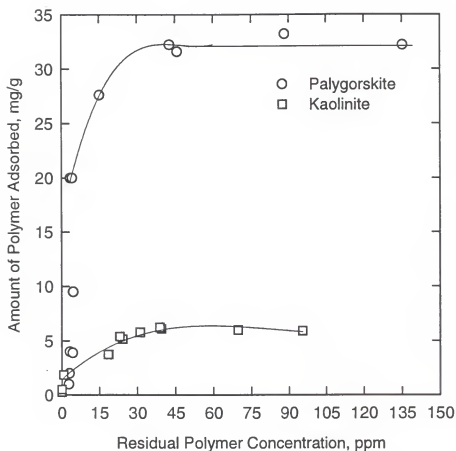


Figure 7.6. Adsorption isotherms of PEO on clays at pH 9.5 (PEO MW = 5,000,000).

the basis of the low PEO adsorption on these silicates. The adsorption density is normalized with respect to the weight of the solids since the layered and chain silicates are porous (see Table 3.6). The saturation adsorption density of PEO on the silicates is summarized in Table 7.2. The use of the BET surface area values is thus seen to underestimate the adsorption density on palygorskite, kaolinite, tremolite and augite. Estimation of the effective surface area, however, is required for comparing adsorption on samples of different porosity and is discussed next.

#### Estimation of the effective surface area

BET method. The hydrodynamic diameter of the molecules of PEO of 5,000,000 MW varies between 91 nm and 225 nm (see Figure 3.2). Therefore, the effective surface area for polymer adsorption is not the total surface area determined from the BET measurements since pores below 91 nm size would be excluded in the adsorption process. Further, the effective surface areas corresponding to these pore diameters will give minimum and maximum values of the saturation adsorption density respectively. The BET surface area for tremolite for pore sizes of 91 nm or higher and 225 nm or higher is 0.297 and 0.023 m<sup>2</sup>/g respectively while for augite and the orthosilicates there is no corresponding detectable surface area. Thus the insensitivity of the BET method to large pore sizes renders it unsuitable for determining effective surface area for higher molecular weight polymers.

Particle size measurements. The geometric surface area calculated from the particle size distribution of the tremolite and augite is about 0.24 m<sup>2</sup>/g. This area is calculated based on the assumption of equivalent spherical particles.

Table 7.2. Saturation adsorption density of PEO (MW = 5,000,000) on chain and orthosilicates.

Material	Flocculation	Saturation Adsorption Density, mg/g
Palygorskite	Yes	32.0
Kaolinite	Yes	6.0
Tremolite	Yes	5.2
Augite	Yes	3.4
Almandine	No	0.4
Olivine	No	0.6
Topaz	No	0.6

The saturation adsorption density of PEO, on this basis, is about 10 and 20 mg/m<sup>2</sup> respectively. These values are an order of magnitude more than the saturation adsorption density of PEO on oxides which exhibited flocculation (see Figure 5.5).

An estimate of the effective surface area of palygorskite was obtained by considering its needle like morphology with the particles typically of 1.0 µm length and 0.05 µm in cross-section [Hog85]. The microporosity of the particles, which comprises of the intralayer channels for an individual crystallite and the interlayer channels between the crystallites, is inaccessible to PEO of 5,000,000 MW. Using the known density of palygorskite (2240 kg/m<sup>3</sup>) an external surface area (the geometric surface area) of about 36 m<sup>2</sup>/g is obtained. This effective surface area corresponds to a saturation adsorption density of about 0.9 mg/m<sup>2</sup> and is similar to those determined for the flocculating oxides viz. SiO<sub>2</sub>, MoO<sub>3</sub> and V<sub>2</sub>O<sub>5</sub>.

Hg-porosimetry. More realistic values of the surface area involved in the adsorption process for tremolite and augite were obtained using Hg-porosimetry (see Table 7.3). Also the saturation adsorption density of PEO, calculated on this basis is reported in Table 7.3. These values are reasonable considering that the saturation adsorption density of PEO of 100,000 MW was determined to be about 4±1.5 mg/m<sup>2</sup> on mica, a sheet silicate [Kle84; Luc90].

In view of the above discussion, even though uncertainties are involved in estimation of the actual surface area involved in the adsorption process, a trend of a higher adsorption of PEO on the chain and layer silicates than the orthosilicates is observed. The higher adsorption density of PEO on the layered and chain

Table 7.3. Estimated surface areas from Hg-porosimetry and the calculated saturation adsorption densities for tremolite and augite.

Material	Effective surface area, $\text{m}^2/\text{g}$		Saturation Adsorption Density, $\text{mg}/\text{m}^2$	
	Pore size (91nm)	Pore size (225nm)	Pore size (91nm)	Pore size (225nm)
Tremolite	1.42	1.00	3.66	5.20
Augite	1.38	0.88	2.46	3.86

silicates than the oxides may be attributed to a different conformation of the PEO molecule on these substrates. AFM studies were conducted on polished samples of these minerals to gain further insight into the conformation of the PEO molecules on chain silicates.

#### AFM Studies of Adsorbed Molecules on Tremolite and Augite

##### Tremolite

The AFM image of the bare tremolite surface is shown in Figure 7.8a. The mean surface roughness was determined to be 0.2 nm while the maximum peak to valley difference is 1.0 nm. The image of the adsorbed PEO (MW = 5,000,000) molecules at pH 9.5 after 1 hour of adsorption is shown in Figure 7.8b. The presence of the polymer on the tremolite surface was corroborated by obtaining images in the friction mode where the adsorbed polymer molecules are characterized by regions of lower friction (see Figure 7.8c) [Cul94]. The histogram of the parking areas of the PEO molecules on tremolite is shown in Figure 7.8d. The interpretation of these images to explain the polymer conformation at the solid-solution interface is given below.

The polymer concentration of 5 ppm was used which corresponds to achieving saturation adsorption density from the results obtained with the solution depletion technique. Although a complete coverage of the surface with the PEO molecules was expected the polymer was adsorbed as a spotty coating, i.e., the surface appears to be unsaturated (see Figures 7.b and c). This observation is not understood at present but significantly different factors from the adsorption experiments using the solution depletion technique such as the lack of turbulence

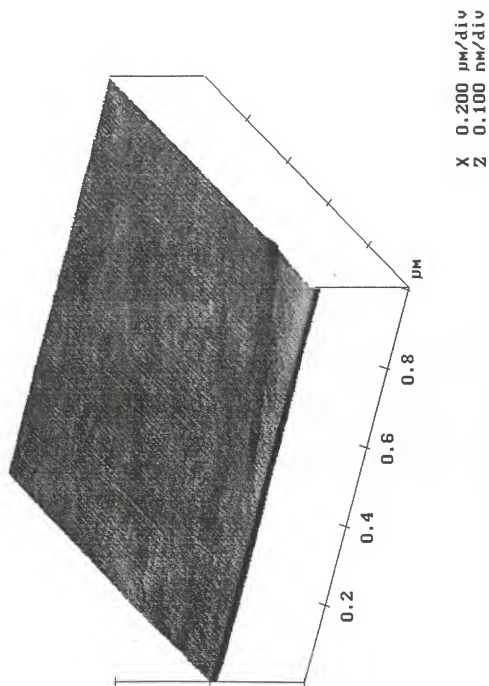


Figure 7.7 AFM image of bare tremolite surface.

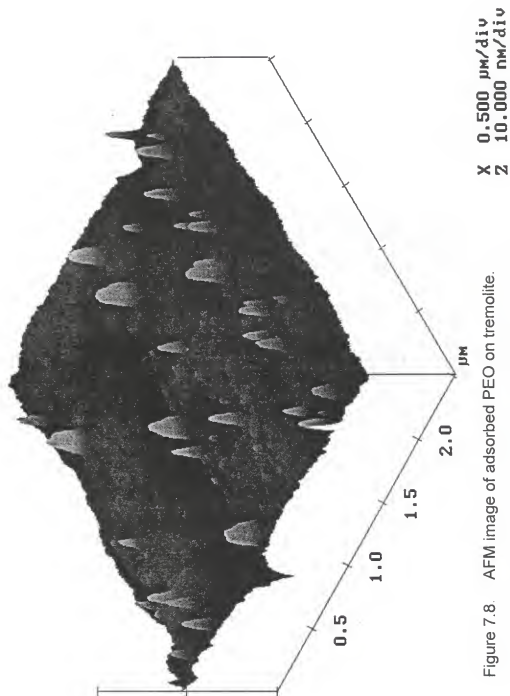


Figure 7.8 AFM image of adsorbed PEO on tremolite.

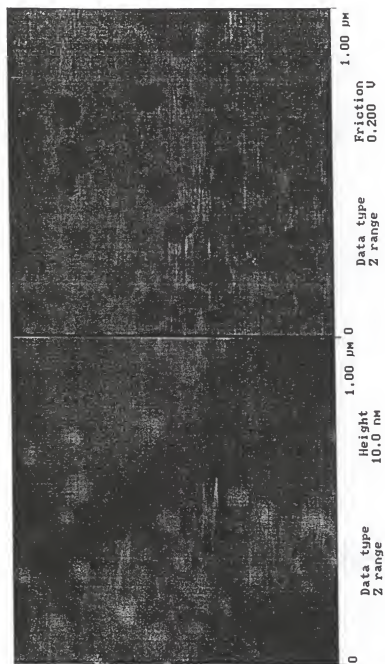


Figure 7.9. AFM Friction image of adsorbed PEO on tremolite.

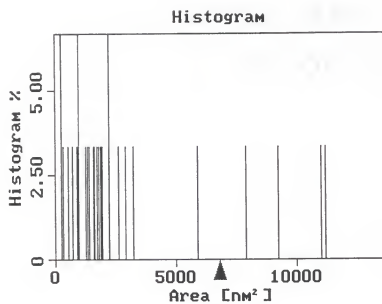


Figure 7.10. Histogram of parking area of PEO molecules on tremolite.

and a flat geometry of the tremolite surface in the AFM may have contributed to this behavior.

The thickness of the adsorbed PEO molecules, as determined from section analysis of Figure 7.8b, is between 2.5-5.0 nm. The maximum and minimum values of the parking area of the PEO molecules, as obtained from Figure 7.8d, are 16,000 and 770 nm<sup>2</sup> respectively and may be due to the polydispersity of the polymer sample. The histogram also revealed that the large molecules are fewer in number than the small molecules. The range of parking areas obtained from the histogram in Figure 7.8d correspond to PEO MW between 300,000 and 4,000,000 from the consideration of a flat conformation, i.e., with all the segments in contact with the surface. The molecular weight distribution of the PEO molecules of 5,000,000 MW in solution, as determined by light scattering, lies in a similar range. Thus the conformation of the adsorbed molecules appears to be flat which is in agreement with the theoretical predictions [Coh84;Cos90]. According to their theory the loops and tails develop only after adsorption of a monolayer of polymer molecules on the substrate. The optimum flocculation dosage is, however, always below the monolayer coverage and the occurrence of a nearly flat conformation seems in apparent contradiction to the predicted and observed conformation. However, the two seemingly opposite observations are explained by considering the dynamics of polymer conformation [Pel90]. The initial attachment of the polymer molecule to the surface is associated with a conformation similar to the random coil in solution and the polymer chain eventually relaxes towards a flat conformation (the equilibrium conformation) as long as the surface is unsaturated. The time scale of the

relaxation process has been estimated to be the order of a few seconds which agrees with the experimental observation that the flocculation is instantaneous. In the present AFM results the experimental observation of the adsorbed polymer is made after an hour during which the polymer molecules would have acquired a flat conformation.

The thickness of the adsorbed PEO molecule on tremolite, from Figure 7.8b indicates a flat conformation. However, as observed from Figure 4.13c the thickness of the same polymer molecules on silica is between 25-50 nm even though the parking areas are similar. Thus the lower thickness could be due to the type of technique used to probe the adsorbed molecule in the AFM. In the contact mode, used for tremolite, the applied force is about two orders of magnitude more than in the tapping mode used for silica, and hence the contact mode is sensitive only to rigid materials. It is known that the segment density distribution of the adsorbed macromolecules falls off exponentially into the solution from the solid/solution interface [Coh84;Cos84]. In such a case, only the incompressible adsorbed polymer molecule, corresponding to the first few layers will be imaged in the contact mode. Further, the lower saturation adsorption density on silica ( $0.63 \text{ mg/m}^2$ ) than tremolite ( $3.66 \text{ mg/m}^2$ ) precludes a flatter adsorption on tremolite than silica. Also, no evidence for multilayer or copious adsorption leading to high adsorption density on tremolite was observed. In this regard, further investigations are warranted to correlate the adsorption studies on a flat plate in the AFM with the solution depletion technique used for adsorption density measurements on powders.

### Augite

The mean roughness of the bare surface of the augite sample shown in Figure 7.9a was determined to be 0.3 nm and the maximum peak to valley difference was found to be 0.8 nm. The image of the adsorbed PEO molecules after 1 hour of adsorption at pH 9.5 is presented in Figure 7.9b. The presence of the adsorbed molecules was also corroborated by obtaining images in the friction mode similar to the case of tremolite (see Figure 7.9c). In contrast to tremolite, a larger number of PEO molecules appear to adsorb on the augite surface, though a complete surface coverage is not observed. The thickness of the incompressible layer of adsorbed polymer (less than 2.5 nm) is observed to be lower than on tremolite. The parking area of the PEO molecules, as indicated from the histogram in Figure 7.9d, was determined to be between 200 and 2,550 nm<sup>2</sup> corresponding to a size distribution between 15-70 nm. These values when compared with those obtained for tremolite indicate a more coiled molecule at the solid/solution interface in the case of augite, and thereby the important role of the surface characteristics in determining the conformation of the adsorbed polymer molecule.

Conceptually, the adsorbed polymer in the form of a random coil invokes the picture of loops and tails in addition to the train segments. The involvement of segments in the formation of loops and tails is expected to result in a decrease in the parking area from a flat conformation of the adsorbed polymer molecule.

An attempt was made to calculate the parking area of adsorbed PEO molecule with a random coil conformation following the model of Tronel-Peyroz [Tro83]. This model was used by Behl et al [Beh93c] to calculate the parking area

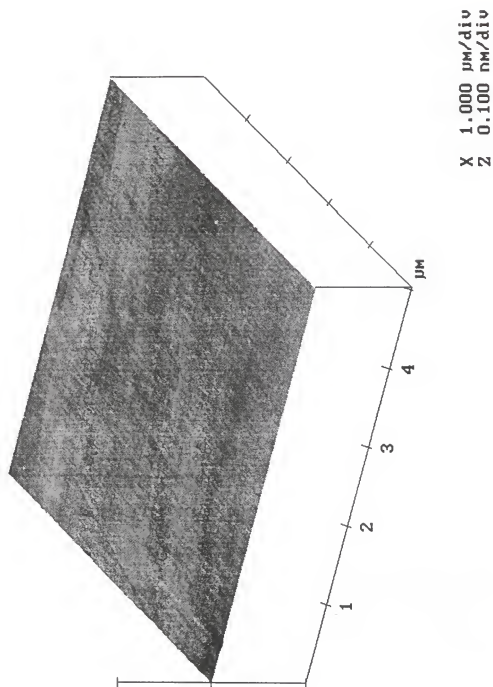


Figure 7.11. AFM image of bare augite surface.

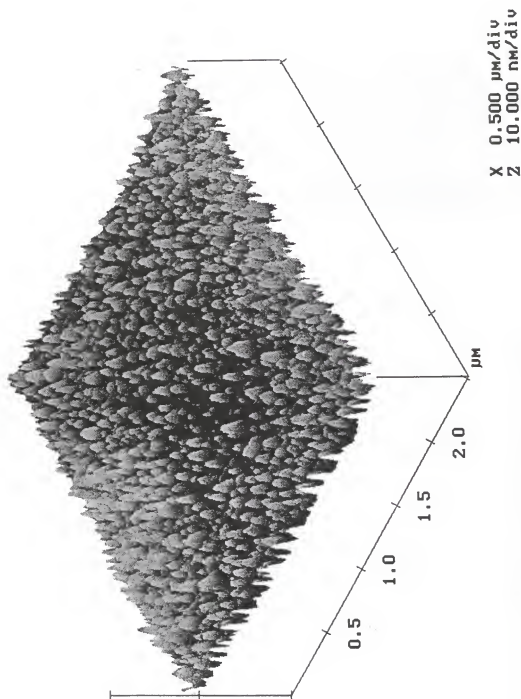


Figure 7.12. AFM image of adsorbed PEO on augite.

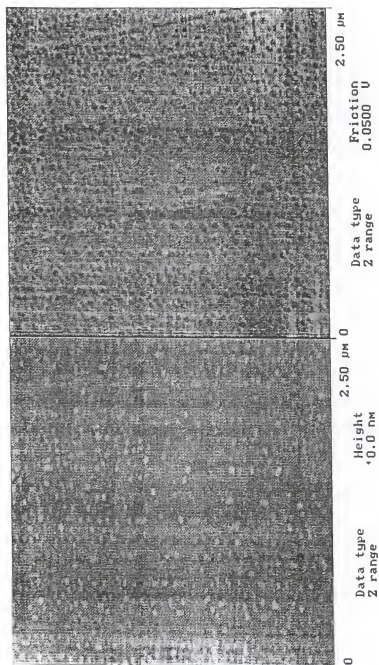


Figure 7.13. AFM Friction image of adsorbed PEO on augite.

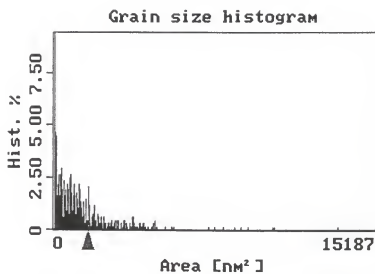


Figure 7.14. Histogram of parking area of PEO molecules on augite.

of the adsorbed PEO molecule in the molecular weight range of 3,400-5,000,000. The calculated parking area, however, predicted a decrease in the saturation adsorption density with increasing molecular weight. The experimental results of Behl et al [Beh93c] for apatite-PEO and dolomite-PEO systems and also of Cohen-Stuart et al [Coh84] for latex-PEO system, however, show an increase in the saturation adsorption density with increasing molecular weight. Their results are in agreement with the predicted effect of molecular weight on saturation adsorption density [Sat80, Daw82, Lip74]. The Tronel-Peyroz model, in addition to predicting a reverse trend of the variation of saturation adsorption density with molecular weight, also calculates a higher parking area than that obtained with the assumption of a flat conformation for PEO of molecular weight higher than 600,000. Thus there is still a critical need for a suitable model for calculating the parking area of adsorbed polymer molecule with a random coil conformation.

The AFM studies showed that the PEO molecules adsorbed at certain sites on the surface even though the initial polymer concentration was high enough to cover the whole surface. This may be an experimental evidence of the concept of active sites proposed by Behl et al [Beh93c] for polymer adsorption since due to surface heterogeneities not all of the surface may be active for polymer adsorption. The chemical binding entities on the surface which comprise the region of an active site have been identified as highly acidic surface hydroxyl groups (Bronsted acid sites) (Chapters 4-6). Further, for silica, the isolated silanols were determined to be the PEO adsorption sites irrespective of pH. The adsorption and flocculation of silicates at pH 9.5 indicates the presence of such groups on silicate surfaces as

well. The surface characterization of the silicates was conducted to elucidate the presence of isolated silanols and other Bronsted acid sites for PEO adsorption.

### Surface Characterization of Silicate Minerals

The DRIFT spectra for the chain and layered silicates are summarized in Figure 7.10 while those for the orthosilicates are summarized in Figure 7.11. The observed positions of the bands in the hydroxyl region are in agreement with those reported by van der Marel and Beutelspacher [van76]

#### Kaolinite

The characteristic bands at  $3696$  and  $3617\text{ cm}^{-1}$  of the structural hydroxyls groups were observed in the DRIFT spectra shown in Figure 7.10. The band at  $3696\text{ cm}^{-1}$  has been attributed to the hydroxyl groups belonging to the octahedral layer but opposite to the tetrahedral oxygens of the adjacent silica layer [Far64]. The band at  $3617\text{ cm}^{-1}$  is due to the hydroxyl groups between the tetrahedral and the octahedral sheets [Far64]. The weaker bands at  $3650$  and  $3670\text{ cm}^{-1}$  have been attributed to the outer surface hydroxyls - the conventional surface hydroxyls - which occur at the broken edges and on the octahedral layer that is exposed to the surface [Hai67]. The hydroxyls responsible for the band at  $3696\text{ cm}^{-1}$  have been considered to be isolated in nature [Grim68].

#### Palygorskite

The band at  $3619\text{ cm}^{-1}$  has been attributed to the isolated hydroxyls by Serna et al [Ser78]. These hydroxyls, however, are not the conventional surface hydroxyls but belong to the structure of palygorskite similar to kaolinite. The water molecule coordinated to the magnesium ion has one unperturbed OH giving rise to the band

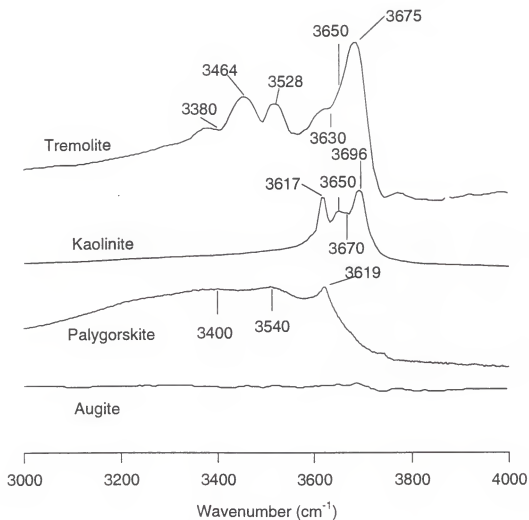


Figure 7.15 DRIFT spectra of the chain and layered silicates in the hydroxyl region

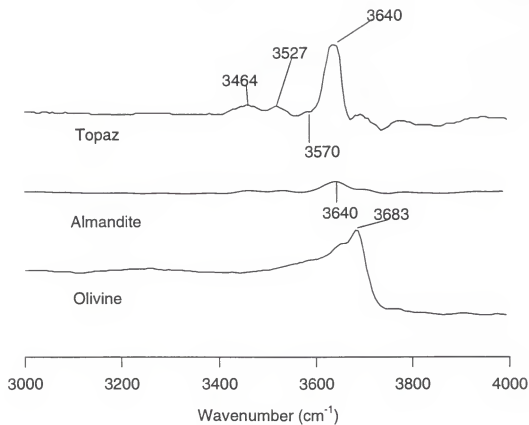


Figure 7.16. DRIFT spectra of orthosilicate minerals in the hydroxyl region.

at  $3619\text{ cm}^{-1}$  while the band at  $3540\text{ cm}^{-1}$  arises due to the hydrogen bonding between the other hydroxyls on the magnesium ion with neighboring hydroxyls. The band at  $3400\text{ cm}^{-1}$  is due to the presence of molecular water hydrogen bonded to the coordinated water molecules on the external surface and the channels inside the palygorskite fibers.

#### Tremolite and Augite

The DRIFT spectra of tremolite shown in Figure 7.10 exhibits several bands in the hydroxyl region which are in agreement with those reported by Marel and Beutelspacher [Mar76]. On the other hand, a featureless spectra was obtained for augite. The presence of (OH) in the amphibole structure is probably responsible for the bands in the hydroxyl region while only surface hydroxyls are possible for augite. The featureless spectra for augite may then due to a low density of surface hydroxyls.

#### Almandite, Topaz and Olivine

The band observed at  $3640\text{ cm}^{-1}$  is attributed to the structural OH for both topaz and almandite (see Figure 7.11). The bands at  $3527$  and  $3464\text{ cm}^{-1}$  for topaz are due to the hydrogen bonded hydroxyls. The spectra of olivine provided in literature is featureless in the hydroxyl region [Mar76]. Therefore, the band at  $3683\text{ cm}^{-1}$  is probably due to an impurity similar to the case of palygorskite coating on being present on the dolomite sample reported by Moudgil et al [Mou95b].

#### Correlation between isolated hydroxyls and adsorption

The different type of hydroxyl groups on the silicate samples along with the saturation adsorption density are summarized in Table 7.4. Augite, which did not

Table 7.4. Type of hydroxyl groups on silicates along with PEO saturation adsorption density.

Material	Flocculation	Saturation Adsorption Density (mg/g)	Type of surface hydroxyl
Palygorskite	Yes	32.0	Isolated Bonded
Tremolite		5.2	Isolated Bonded
Augite		3.4	-
Almandite	No	0.4	Isolated
Topaz		0.6	Isolated
Olivine		0.6	Isolated Bonded

exhibit isolated hydroxyls, showed a significant amount of PEO adsorption while the orthosilicates which all exhibited the isolated hydroxyls showed lower adsorption than augite. Thus, similar to the case of oxides, the presence of isolated hydroxyls on silicate minerals did not always result in significant PEO adsorption.

#### Adsorption Mechanism(s) of PEO on Silicates

An obvious difference between the flocculating and the non-flocculating silicates is the structure of the silicate itself. The chain and layered silicates exhibit connectivity of the silicate tetrahedra in one- and two-dimensions respectively and show a significantly higher adsorption of PEO than the orthosilicates which have silicate tetrahedra isolated from each other through the presence of octahedral cavities containing divalent or trivalent atoms. It has been shown earlier that the presence of Bronsted acid sites strong enough to bind the ether oxygen of PEO is essential for adsorption of PEO. The relation between the structure of the silicates and the resultant Bronsted acidity is discussed next.

#### Layered silicates

The surface of the layered silicates consists of broken bonds at the edges, hydroxyl groups which are part of the structure, and the exchangeable ions which may be coordinated to the former two sites but mainly occur to maintain electroneutrality of the tetrahedral or the octahedral layer, when ions of lower valence than Si or Al are substituted respectively.

The Al may substitute for Si in the silicate layer resulting in enhanced acidity of the adjacent SiOH groups. This occurs due to a strong attraction of the bridging oxygen between the Al and Si towards Al, which increases the attraction of the

terminal oxygen on SiOH to Si and weakening of the O-H bond [Hai67]. Interestingly, the frequency of the isolated silanol in the mixed oxide system was determined to be the same as on silica,  $3747\text{ cm}^{-1}$ .

In the clays, the isomorphous substitution of Al for Si leading to enhanced acidity of the silanol group occurs at the edges only since the layer consists of an essentially siloxane surface. However, the replacement of Al for Si in the siloxane layer results in a negative charge which is balanced by the exchangeable cation. The exchangeable cation by itself is a Lewis acid but due to the presence of a hydration layer around the exchangeable ion this acidity is transformed to Bronsted acidity. This has been attributed to the submission of the hydration layer to a strong polarizing field due to the small radius of curvature of the cation, as compared with the quasi-infinite radius of curvature of the anionic siloxane sheet [Fri90]. The high strength of the Bronsted acid sites comprising of hydrated exchangeable cations and the edge OH groups is well documented through spectroscopic studies involving pyridine adsorption and titration with indicator dyes [Rup 87, Fri90, Sch95].

The flocculation of montmorillonite, a layered silicate, with PEO has been shown to be strongly dependent on the type of exchangeable cation present by Scheiner and co-workers [Sch86;Sch87;Bro89]. They suggested that the exchangeable ion with its hydration shell constitutes the binding sites for the ether oxygen of PEO. Their proposed adsorption mechanism is illustrated in Figure 12. However, the flocculation of palygorskite was not significantly affected by the type of exchangeable cation [Sch86]. This is expected since the primary source of the

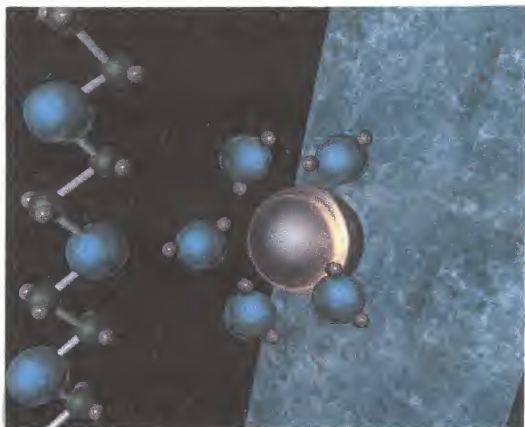


Figure 7.17. Adsorption of PEO on clays by interaction of the ether oxygen of PEO with the hydration shell of the exchangeable ion (Bronsted acid site) (after [Sch86]).

exchangeable ions on palygorskite has been suggested to be different than on montmorillonite [Gri68].

The exchangeable cations on the montmorillonite surface arise as a result of isomorphous substitution of Al for Si in the basal planes, as mentioned above. The exchangeable cations which are present inside the tactoid are inaccessible to the high molecular weight PEO molecules. The increase in the tactoid thickness is in the reverse order of the polarizing power of the cations and is accompanied by a decrease in the external surface area available for PEO adsorption. Hence, a significant lower dosage was required for flocculation of a Ca-montmorillonite than Na-montmorillonite [Sch86].

In palygorskite, the edges constitute most of the external surface area in contrast to kaolinite and montmorillonite. The edges consist of the broken bonds of Si-O-Si type which compensate their residual charge by forming isolated silanol groups with a spacing of about 0.5 nm [Rau87]. The edges which form the periphery of the palygorskite fibers are also the main source of the exchangeable cations. Their absence in the internal structure of the fiber renders the flocculation of palygorskite relatively insensitive to the type of exchangeable cation.

The other source of isolated hydroxyls in palygorskite is the coordinated water molecule attached to the magnesium ion. Exposed magnesium ions may play a similar role as the exchangeable cations in montmorillonite when the coordinated water is replaced. The structural hydroxyls are accessible only at the faces of the (100) plane which constitutes a small fraction of the available surface area. This is because of the dimensions of the face being less than typically 1/10 th of the fiber

length. The predominant adsorption of PEO on the edges is indicated by alignment of the needles in the flocs [Hog85].

#### Chain silicates

The pyroxene (augite) and amphibole (tremolite) type of silicates do not have a significant ion-exchange capacity. Their fibrous morphology, similar to palygorskite, presents the Si-O-Si broken bonds at the surface which can satisfy the valence by formation of SiOH type of groups. This continuity of SiOH type of sites is lost in the orthosilicates where the silicate tetrahedra are isolated. The influence of the polymerization of SiO<sub>4</sub> tetrahedra on the acidity of these SiOH groups needs to be investigated. The adsorption of PEO on tremolite and augite indicates that SiOH groups are more acidic than on the orthosilicates, and are close in acidity to the SiOH on layered silicates.

The surface characterization of the silicate samples revealed that strong Bronsted sites capable of interaction with the ether oxygen of PEO were present only on layered and chain silicates such as kaolinite, palygorskite, tremolite and augite. The presence of such strong Bronsted sites seems to be related to the connectivity of the silicate tetrahedra since the orthosilicates did not exhibit significant PEO adsorption. Thus the adsorption mechanism for PEO determined on silica was shown to be the same for mixed oxides containing silica.

## CHAPTER 8

### CONCLUSIONS AND FUTURE WORK

#### Summary

The specificity of hydrogen bonding of the ether oxygen of PEO with the surface hydroxyls (Bronsted sites) has been established in this study. The acidity of the Bronsted sites is the parameter that determines the interaction with the ether oxygen of PEO, a Lewis base. The strength of the Bronsted acid sites on oxide samples was characterized by their point of zero charge and vibrational characteristics of adsorbed pyridine, a weak base. It was determined that highly acidic oxides of the type  $MO_3$ ,  $M_2O_5$  and  $MO_3 \cdot nH_2O$  such as  $MoO_3 \cdot 2V_2O_5$ , and  $SiO_2$  strongly adsorb and flocculate with PEO.  $TiO_2$ , an  $MO_2$  type of oxide, did not adsorb PEO due to weaker acidity of the Bronsted sites than the silanols.

It was shown that the common feature of the previously identified PEO binding sites, the isolated silanols on silica and exchangeable ions on clays, is the acid strength of these sites. The Bronsted acid sites on clays also consists of the exchangeable ions besides the isolated hydroxyls. The concept of the strength of the Bronsted acid sites governing the interaction with the ether oxygen of PEO thus explained all the previous and present observations made regarding the adsorption sites of PEO on oxide and silicate surfaces.

This study also revealed that the presence of isolated surface hydroxyls, a criterion extrapolated from adsorption studies on silica/non-ionic polymer system, is not sufficient to explain adsorption of PEO on oxide surfaces. The acidity of isolated silanols arises from the nature of the silica surface. The oxides bearing isolated hydroxyls on the surface, e.g., alumina, titania, magnesia and hematite did not exhibit measurable PEO adsorption. On the other hand crystalline silica,  $\text{MoO}_3$  and  $\text{V}_2\text{O}_5$  which did not exhibit the isolated hydroxyls in their spectra showed significant PEO adsorption. Similarly, for the silicate samples examined no correlation between the presence of isolated surface hydroxyls and PEO adsorption was observed.

The specificity of hydrogen bonding of isolated silanols with polar organic molecules such as diethyl ether, the monomer unit of PEO, has been established for the case of adsorption from the vapor state [Kis65]. In the present study it was determined that the specificity of hydrogen bonding interaction between the isolated silanols and the ether oxygen of PEO persists in the presence of an aqueous medium. The presence of water molecules, however, precludes this interaction to be observed by infrared spectroscopy. The observation of only the isolated silanols in the DRIFT spectra of silica pretreated at  $1100^\circ\text{C}$  along with significant adsorption of PEO on this sample indicated that the isolated silanols are indeed the principal binding sites for the ether oxygen of PEO.

The isolated silanols were shown to be the stable surface sites for PEO adsorption with respect to pH. The adsorption of PEO on silica A, which exhibited isolated silanols, was insensitive to pH in the range 3.0 to 9.5. On the other hand, PEO adsorption was significantly reduced on silica B, which did not exhibit the

isolated silanols, when the pH was changed from 3.0 to 9.5. The desorption of high molecular weight PEO molecules from a fused silica plate was shown to occur by AFM studies when the pH was changed in-situ from 3.0 to 9.5.

The adsorption of PEO on silica B and silica plate surface near the isoelectric point of pH 2.0, however, indicated that silanols other than the isolated type are capable of hydrogen bonding with the ether oxygen of PEO. It is suggested that their low concentration and higher acidity compared to the isolated silanols results in significant ionization of these sites with increasing pH and thus a concomitant loss of PEO adsorption sites. The electrokinetic and PEO adsorption studies on silica B support this hypothesis. Further compelling evidence, showing the loss of PEO binding sites accompanied by an increasingly negatively charged surface on a silica plate, was illustrated in the AFM studies. The desorption of PEO molecules upon changing the pH from 3.0 to 9.5 was corroborated by the force/distance profiles which changed from that for a pure steric repulsion to completely electrostatic repulsion for the same pH change. The AFM investigations thus showed that previous hypotheses regarding the observed decrease in adsorption of non-ionic polymers like PEO with increasing pH such as 1) a negatively charged surface repels PEO molecules and 2) the hydrated counter ions prevent the approach of PEO to the silica surface are not correct.

The surface acidity of the oxides and silicates may also arise from the presence of Lewis acid sites. Among the oxides investigated in the present study the strongest Lewis acid sites have been demonstrated on the alumina surface [Dav90]. The heat pretreatment of alumina, which resulted in a partially

dehydroxylated surface and an increased concentration of Lewis acid sites, was found not to affect the PEO adsorption significantly. It appears, therefore, that the Lewis acid sites do not play a major role in PEO adsorption, a conclusion also supported by the investigations of van der Beek et al [van91].

The dehydroxylation process also mitigates the accessibility of the Bronsted acid sites on the alumina surface to the PEO molecules. However, the PEO adsorption was not affected significantly indicating that the lack of accessibility to the surface sites is not the reason for negligible PEO adsorption on alumina. It is the presence of Bronsted sites of weaker acidity than the silanols on the alumina surface which results in an insignificant adsorption of PEO on alumina.

The Bronsted acid sites on silicates capable of binding the ether oxygen of PEO were shown to be related to the connectivity of the  $\text{SiO}_4$  tetrahedra in chains or layers. Thus layered silicates such as kaolinite and palygorskite and chain silicates such as pyroxenes (augite) and amphiboles (tremolite) were shown to adsorb PEO while the orthosilicates such as olivine, almandite and topaz did not exhibit PEO adsorption.

The other suggested PEO adsorption mechanisms in the literature such as the presence of adsorbed surface ions, which in solution state are capable of complexing with the ether oxygen, and positively charged surface sites do not play a major role in the adsorption process. The presence of sodium ions on the alumina B surface and precipitation of Mo ions on alumina and titania did not affect the adsorption of PEO on these surfaces. Also, predominance of positively charged surface sites on alumina or hematite at pH 3.0 did not result in significant PEO

adsorption. On the other hand, the high negative charge on the surface of silica A,  $\text{MoO}_3$  and  $\text{V}_2\text{O}_5$  did not preclude PEO adsorption.

#### Suggestions for Future Work

The concept of the specificity of hydrogen bonding of PEO with the surface hydroxyls need to be extended to other non-ionic polymers such as PVA and polyacrylamide (PAM). The behavior of PVA/silica system has been shown to be similar to the PEO/silica system[Tad78, Kha88]. PAM is known to be a stronger flocculant than both PEO and PVA [Sch87]. This indicates that the surface/segment interactions for PAM are stronger than PEO and PVA. The quantification of the substrate-polymer-solvent interactions needs to be developed to predict the adsorption behavior at the solid/solution interface.

The characterization of adsorption sites on oxides was accomplished through electrokinetic studies and infrared spectroscopy of adsorbed pyridine. However, determination of the concentration and strength distribution of surface sites will be of value in identifying methods to create the appropriate sites for polymer adsorption. For example, Stober silica and crystalline silica exhibited different PEO adsorption with respect to pH which was attributed to the presence of isolated silanols only on Stober silica. The elucidation of the surface structure of the two silica samples by molecular modeling and experimental techniques is necessary for developing of pretreatments that can result in the formation of isolated silanols on crystalline silica.

In addition to elucidation of the surface structure and the distribution and reactivity of surface sites, molecular modeling of the polymer molecules will offer

valuable insight into the adsorption process. The combined knowledge of the molecular architecture of the surface and reactivity of the different possible adsorption sites along with the chemistry of the polymer molecules will be useful in synthesis/identification of an appropriate polymer for a given particulate system.

The potential of AFM to investigate the microstructure at the solid/solution interface in the system of interest has been demonstrated in this study. The cause of the high saturation adsorption density of PEO determined on the layered and chain silicates was investigated through AFM studies. Although no explanation at present seems to exist, information on PEO conformation on a flat surface was obtained. The polymer appeared to adsorb with a flatter conformation on tremolite than augite as indicated by the AFM image analysis. A definite comparison between the parking area of the adsorbed polymer molecules and their size in solution could not be made due to the polydispersity of the polymer samples. It is suggested that further detailed investigations with monodisperse polymers can reveal useful quantitative information on polymer conformation at the solid/liquid interface. A comparison of the experimental data so obtained with the theoretical predictions will lead to a better understanding of the adsorbed polymer layer conformation and subsequent control of the stability of suspensions.

## REFERENCES

- [Ana87] Ananthapadmanabhan, K.P. and Goddard, E.D., "Aqueous Bi-Phase Formation of Polyethylene Oxide-Inorganic Salt Systems," *Langmuir*, 3(1), pp. 25-31, (1987).
- [And 65a] Anderson, J.H., Jr., "Calorimetric vs. Infrared Measures of Adsorption Bond Strengths on Silica," *Surface Science*, 3, pp. 290-291, (1965).
- [And82] Anderson, M.A., and Rubin, A.J., Adsorption of Inorganics at Solid/Liquid Interface, Ann Arbor Science Publishers, Ann Arbor, MI, USA, (1981).
- [And65b] Anderson, P.J., Horlock, R.F., and Oliver, J.F., "Interaction of Water with the Magnesium Oxide Surface," *Transactions of the Faraday Society*, 61, pp. 2754-2762, (1965).
- [Arm69] Armistead, C.G., Tyler, A.J., Hambleton, F.H., Mitchell, S.A., and Hockey, J.A., "The Surface Hydroxylation of Silica," *Journal of Physical Chemistry*, 73, pp. 3947-3953, (1969).
- [Att87] Attia, Y.A., "Design of Selective Polymers for Biological and Colloid Separation by Selective Flocculation," in *Flocculation in Biotechnology and Separation Systems*, Ed., Attia, Y.A., Elsevier Science Publishers, pp. 297-308, (1987).
- [Bai76] Bailey Jr., F.E., and Koleske, J.V., Poly(ethylene oxide), Academic Press, New York, (1976).
- [Bas61] Basila, M.R., "Hydrogen Bonding Interaction Between Adsorbate Molecules and Surface Hydroxyl Groups on Silica," *Journal of Chemical Physics*, 35(4), pp. 1151-1158, (1961).
- [Beh93a] Behl, S., "Controlled Polymer Adsorption for Enhanced Selectivity in flocculation," Ph.D. Thesis, University of Florida, Gainesville, FL, USA, (1993).
- [Beh93b] Behl, S., Moudgil, B.M., and Prakash, T.S., "Control of Active Sites in Selective Flocculation -Part I: A Mathematical Model", *Journal of Colloid and Interface Science*, 161, pp. 414-421, (1993).

- [Beh93c] Behl, S. and Moudgil, B.M., "Role of Active Sites in Flocculation - Concept of Equivalent Active Sites", *Journal of Colloid and Interface Science*, 161, pp. 437-442, (1993).
- [Beh93d] Behl, S., and Moudgil, B.M., "Mechanisms of Polyethylene Oxide Interaction with Apatite and Dolomite", *Journal of Colloid and Interface Science*, 161, pp. 443-449, 1993.
- [Ber94] Berhouet, S., and Toulhoat, H., "Nature of Acidic Sites of the Lewis Type at the surface of Mica and related Aluminosilicate Materials," *Langmuir*, 10, pp. 1832-1836, (1994).
- [Bla90] Blaakmeer, J., "The Adsorption of Weak Polyelectrolytes and Polyampholytes," Ph.D. Thesis, Agricultural University, Wageningen, The Netherlands, (1990).
- [Bri90] Brinker, C.J., and Scherer, G.W., Sol-Gel Science: The Physics and Chemistry of Sol-Gel Processing, Academic Press, Boston, MA, USA, (1990).
- [Bro89] Brown, P.M., Stanley, D.A., and Scheiner, B.J., "An explanation of flocculation using Lewis acid-base theory", *Minerals and Metallurgical Processing*, pp. 196-200, (1989).
- [Car94] Carniti, P., Gervasini, A., Auroux, A., "Energy Distribution of Surface Acid Sites of Metal Oxides," *Journal of Catalysis*, 150, pp. 274-283, (1994).
- [Cha86] Chanchani, R., "Selective Flotation of Dolomite from Apatite Using Sodium Oleate as the Collector," Ph.D. Thesis, University of Florida, Gainesville, FL, USA, (1986).
- [Cha63] Chapman, I.D. and Hair, M.L., "The Role of the Surface Hydroxyl Groups in Catalytic Cracking," *Journal of Catalysis*, 2, pp. 145-148, (1963).
- [Che85] Cheng, Y.C., "The Effect of Surface Hydration on the Adsorption and Flocculation of a Model Silica Suspension Using Polyethylene Oxide," M.S. Thesis, University of Florida, Gainesville, Florida, USA, (1985).
- [Che59] Chessick, J.J., and Zettlemoyer, A.C., "Heats of Immersion of Solids in Liquids," *Advances in Catalysis*, 11, pp. 263-286, (1959).

- [Chr93] Chronister, C.W., and Drago, R.S., "Determination of Hydrogen-Bonding Acid Sites on Silica using the Cal-Ad Method," *Journal of the American Chemical Society*, 115, pp. 4793-4798, (1993).
- [Coh84] Cohen-Stuart, M.A., Waajen, F.H.W.H., Cosgrove, T., Vincent, B., and Crowley, T.L., "Hydrodynamic Thickness of adsorbed Polymer Layers," *Macromolecules*, 17(9), pp. 1825-1830, (1984).
- [Cos84] Cosgrove, T., Vincent, B., Crowley, T.L., and Cohen Stuart, M.A., "Segment Density Profiles of Adsorbed Polymers," in Polymer Adsorption and Dispersion Stability, Eds. Goddard, E.D., and Vincent, B., American Chemical Society, Washington, D.C., pp.147-159, (1984).
- [Cos90] Cosgrove, T., "Volume Fraction Profiles of Adsorbed Polymers," *Journal of Chemical Society Faraday Transactions*, 86(9), pp. 1323-1332, (1990).
- [Cow83] Cowell, C. And Vincent, B., "Flocculation Kinetics and Equilibria in Sterically Stabilized Dispersions," *Journal of Colloid and Interface Science*, 95(2), pp.573-582, (1983).
- [Cul94] Cullen, D.C., and Lowe, C.R., "AFM Studies of Protein Adsorption", *Journal of Colloid and Interface Science*, 166, pp.102-108, (1994).
- [Dav90] Davydov, A.A., "Infrared Spectroscopy of Adsorbed Species on the Surface of Transition Metal Oxides," Ed. Rochester, C.H., John Wiley & Sons, New York, (1990).
- [deG81] de Gennes, P.G., "Polymer Solutions Near an Interface I: Adsorption and Depletion Layers," *Macromolecules*, 14, pp. 1637-1644, (1981).
- [deG82] de Gennes, P.G., "Polymers at an Interface II: Interaction between Two Plates Carrying Adsorbed Polymer Layers," *Macromolecules*, 15, pp.492-500, (1982).
- [deG87] de Gennes, P.G., "Polymers at an Interface; a Simplified View," *Advances in Colloid and Interface Science*, 27, pp. 189-209, (1987).
- [Dow92] Dow, J.H., "Dispersion of Ceramic Powders in Ceramic Melts," PhD Thesis, University of Florida, Gainesville, Florida, USA, (1992).
- [Eva73] Evans, R., and Napper, D.H., "Flocculation of Latices by Low Molecular Weight Polymers," *Nature*, 246, pp. 34-35, (1973).

- [Far64] Farmer, V.C., and Russel, J.D., "The Infra-red Spectra of Layer Silicates," *Spectrochimica Acta*, 20, pp. 1149-1173, (1964).
- [Feh89] Feher, F.J., Newman, D.A., and Walzer, J.F., "Silsesquioxanes as Models for Silica Surfaces," *Journal of American Chemical Society*, 111, pp. 1741-1748, (1989).
- [Feh90] Feher, F.J., and Newman, D.A., "Enhanced Silylation Reactivity of a Model for Silica Surfaces," *Journal of American Chemical Society*, 112, pp. 1931-1936, (1990).
- [Fle83] Fleer, G.J., and Lyklema, J., "Adsorption of Polymers," in Adsorption from Solution at Solid/Liquid Interface, Eds. Parfitt, G.D., and Rochester, C.H., Academic Press, London, pp. 153-222, (1983).
- [Fri62] Fripiat, J.J., and Uytterhoeven, J., "Hydroxyl Content in Silica Gel Aerosil," *Journal of Physical Chemistry*, 66, pp.800-805, (1962).
- [Fri90] Fripiat, J.J., "Surface Activities of Clays," in Spectroscopic Characterization of Minerals and Their Surfaces, Coyne, L.M., McKeever, W.S., and Blake, D.F., eds., American Chemical Society, Washington, DC, USA, pp.360-377, (1990).
- [Gra93] Graabe, A., and Horn, R.G., "Double-Layer and Hydration Forces Measured between Silica Sheets Subjected to Various Surface Treatments," *Journal of Colloid and Interface Science*, 157, pp.375-383, (1993).
- [Gre72a] Greenland, D.J., "Interactions between organic polymers and inorganic soil particles," *Mededelingen Fakulteit Landbouwwetenschappen Rijksuniversiteit Gent*, 37, pp.897-914 (1972).
- [Gre72b] Greenland, D.J., "Interactions between organic polymers and inorganic soil particles," *Mededelingen Fakulteit Landbouwwetenschappen Rijksuniversiteit Gent*, 37, pp.915-922, (1972).
- [Gri68] Grim, R.E., Clay Mineralogy, McGraw Hill Inc., New York, NY, USA (1968).
- [Hai67] Hair, M.L., Infrared Spectroscopy in Surface Chemistry, Marcel Dekker, New York, NY, USA, (1967).
- [Hea65] Healy, T.W., and Fuerstenau, D.W., "The Oxide-Water Interface-Interrelation of the Zero Point of Charge and the Heat of Immersion," *Journal of Colloid Science*, 20, pp. 376-386, (1965).

- [Hog85] Hoghooghi, B., "Flocculation of Palygorskite Suspensions and the Orientation of Particle in Flocs," M.S. Thesis, University of Florida, Gainesville, FL, USA, (1985).
- [How67] Howard, G.J., and McConell, P., "Adsorption of Polymers at the Solid Solution Interface," *Journal of Physical Chemistry*, 71(9), pp. 2974-2980, (1967).
- [Ile71] Iler, R.K., The Chemistry of Silica, John Wiley and Sons, New York, NY, USA, (1971).
- [Ile75] Iler, R.K., "The Effect of Surface Aluminosilicate Ions on the Properties of Colloidal Silica," *Journal of Colloid and Interface Science*, 55(1), pp. 25-34, (1975).
- [Iwa82] Iwasaki, I., and Lipp, R.J., in Interfacial Phenomena in Mineral Processing, eds. Yarar, B., and Spottiswood, D.J., Engineering Foundation, New York, NY, pp. 321, (1982).
- [Kha88] Khadilkar, C.S., "The Effect of Adsorbed Poly(vinyl alcohol) on the Properties of Model Silica Suspensions," Ph.D. Thesis, University of Florida, Gainesville, Florida, USA, (1988).
- [Kho84] Khosla, N.K., Bhagat, R.P., Gandhi, K.S., and Biswas, A.K., "Calorimetric and Other Interaction Studies on Mineral-Starch Adsorption System," *Colloids and Surfaces*, 8, pp. 321-336, (1984).
- [Kin76] Kingery, W.D., Introduction to Ceramics, Second Edition, John Wiley & Sons, Inc., New York, NY, USA, (1976).
- [Kis65] Kiselev, A.V., "Calorimetric vs. Infrared Measurements of Adsorption Bond Strengths of Molecules of Different Electronic Structure on Hydroxylated Silica Surface," *Surface Science*, 3, pp. 292-293, (1965).
- [Kje81] Kjellander, R., and Florin, E., "Structure of Polyethylene Oxide in Water," *Journal of Chemical Society, Faraday Transaction I*, 77, pp. 2053, (1981).
- [Kle84] Klein, J., "Forces Between Two Adsorbed Poly(ethylene oxide) Layers in a Good Aqueous Solvent in the Range 0-150 nm," *Macromolecules*, 17, pp. 1041-1048, (1984).

- [Kok90] Koksai, E., Ramachandran, R., Somasundaran, P., and Maltesh, C., "Flocculation of Oxides using Poly(ethylene oxide)," *Powder Technology*, 62, pp. 253-259, (1990).
- [Kun89] Kung, H.H., Transition Metal Oxides: Surface Chemistry and Catalysis, Elsevier, Amsterdam, The Netherlands, (1989).
- [Luc90] Luckham, P.F., and Klein, J., "Force between Mica Surfaces Bearing Adsorbed Homopolymers in Good Solvents," *Journal of Chemical Society Faraday Transactions*, 86(9), pp. 1363-1368, (1990).
- [Mor76] Morterra, C., Ghiotti, G., Garrone, E., and Bocuzzi, F., "Infrared Spectroscopic Characterization of the  $\alpha$ - $\text{Al}_2\text{O}_3$  Surface," *Journal of Chemical Society, Faraday Transactions 1*, 72, pp.2722-2734, (1976).
- [Mor68] Mortland, M.M., and Raman, K.V., "Surface Acidity of Smectites in Relation to Hydration, Exchangeable Cation and Structure," *Clays and Clay Minerals*, 16, pp. 393-398, (1968).
- [Mou91] Moudgil, B.M., and Behl, S., "A Model of the Selective Flocculation Process," *Journal of Colloid and Interface Science*, 146(1), pp.1-8, (1991).
- [Mou92] Moudgil, B.M., Behl, S., and Kulkarni, N., "Measurement of Heat Adsorption of Polyethylene Oxide on Dolomite, Silica and Alumina by Microcalorimetry," *Journal Colloid Interface Science*, 148(2), pp. 337-342, (1992).
- [Mou95a] Moudgil, B.M., Mathur, S., and Behl, S., "Dolomite-Dolomite Separation by Selective Flocculation Technique," *Minerals and Metallurgical Processing*, 12 (1), pp. 24-27, (1995).
- [Mou95b] Moudgil, B.M., Mathur, S. and Behl, S., "Flocculation Behavior of Dolomite With Poly(ethylene-oxide)," *Minerals and Metallurgical Processing*, 12(4), pp. 219-224, (1995).
- [Oka88] Okamoto, Y., and Imanaka, T., "Interaction Chemistry between Molybdena and Alumina: Infrared Studies of Surface Hydroxyl groups and Adsorbed Carbondioxide on Aluminas Modified with Molybdate, Sulfate, or Fluorine Atoms," *Journal of Physical Chemistry*, 92, pp. 7102-7112, (1988).
- [Par65] Parks, G.A., "Isoelectric Points of Solid Oxides, Solid Hydroxides and Aqueous Hydroxo Complex Systems," *Chemical Review*, 65, pp. 177-197, (1965).

- [Par63] Parry, E.P., "An Infrared Study of Pyridine Adsorbed on Acidic Solid-Characterization of Surface Acidity", *Journal of Catalysis*, 2, pp. 371-379, (1963).
- [Pau63] Pauling, L, Nature of the Chemical Bond, Cornell University Press, Ithaca, New York, USA, (1963).
- [Pel90] Pelssers, E.G.M., Cohen Sturat, M.A., and Fleer, G.J., "Kinetics of Bridging Flocculation-Role of Relaxations in the Polymer Layer," *Journal of Chemical Society, Faraday Transactions*, 86(9), pp. 1355-1361, (1990).
- [Pra91] Pradip, "On the Design of Selective Reagents for Mineral Processing Applications," *Metals, Materials & Processes*, 3 (1), pp. 15-36, (1991).
- [Pra96] Prakash, T.S., "Separation of Salts Using Polymer Bi-Phase System," M.S. Thesis, University of Florida, Gainesville, Florida, USA, (1996).
- [Pri71] Primet, M., Pichat, P., and Mathieu, M.V., "Infrared Study of the Surface of Titanium Dioxides, I. Hydroxyl Groups," *Journal of Physical Chemistry*, 75(9), pp. 1216-1220, (1971).
- [Ram89] Ramachandran, R., and Somasundaran, P., "Polymer Surfactant Interactions in bulk and at the Solid/Liquid Interface", in Flocculation and Dewatering, eds. Moudgil, B.M., and Scheiner, B.J., Engineering Foundation, New York, United Engineering Trustees, Inc., New York, NY, (1989).
- [Rau87] Raussell-Colom, J.A., and Serratosa, J.M., "Reactions of Clays with Organic Substances," in Chemistry of Clays and Clay Minerals, ed. Newman, A.C.D., John Wiley & Sons, New York, NY, USA, pp. 371-422, (1987).
- [Ree88] Reed, J.S., Principles of Ceramic Processing, John Wiley & Sons Inc., New York, NY, USA, (1988).
- [Rob64] Robinson, M., Pask, J.A., and Fuerstenau, D.W., "Surface Charge of Alumina and Magnesia in Aqueous Media," *Journal of the American Ceramic Society*, 47(10), pp. 516-520, (1964).
- [Roc76] Rochester, C.H., "Infrared Spectroscopic Studies of Powder Surfaces and Surface-Adsorbate Interactions Including the Solid/Liquid Interface. A Review," *Powder Technology*, 13, pp. 157-176, (1976).

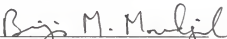
- [Rub76] Rubio, J. and J.A. Kitchener, "The Mechanism of Adsorption of Poly(Ethylene Oxide) Flocculant on Silica," *Journal of Colloid and Interface Science*, 57(1), pp. 132-141, (1976).
- [Rup87] Rupert, J.P., Granquist, W.T., and Pinnavaia, T.J., "Catalytic Properties of Clay Minerals," in Chemistry of Clays and Clay Minerals, ed. Newman, A.C.D., John Wiley & Sons, New York, NY, USA, pp. 275-314, (1987).
- [Sch82] Scheutjens, J.M.H.M., and Fleer, G.J., "Adsorption of Interacting Oligomers and Polymers at an Interface," *Advances in Colloid and Interface Science*, 16, pp. 341-359, (1982).
- [Sch86] Scheiner, B.J. and Stanley, D.A., "Flocculation of fine particles with polyethylene oxide: a proposed mechanism", *Transactions of the Society of Mining Engineers of AIME*, 280, pp. 2115-2117, (1986).
- [Sch87] Scheiner, B.J. and Wilemon, G.M., "Applied Flocculation Efficiency: A Comparison of Polyethylene Oxide and Polyacrylamide," in Flocculation in Biotechnology and Separation Systems, Ed. Attia, Y.A., Elsevier Science Publishers, Amsterdam, pp. 175-186, (1987).
- [Sch95] Schoonheydt, R.A., "Clay Mineral Surfaces," in Mineral Surfaces, eds. Vaughan, D.J., and Patrick, R.A.D., Chapman & Hall, London, England, pp. 303-332, (1995).
- [Ser77] Serna, C, VanScoyoc, G.E., and Ahlrichs, J.L., "Hydroxyl Groups and Water in Palygorskite," *American Mineralogist*, 62, pp. 784-792, (1977).
- [Sha86] Shah, B.D., "Selectivity in Mixed Mineral Flocculation: Apatite-Dolomite System," M.S. Thesis, University of Florida, Gainesville, FL, USA, (1986).
- [Spe92] Sperling, L.H., Introduction to Physical Polymer Science, Second edition, John Wiley & Sons, Inc., NY, USA, (1992).
- [Tad78] Tadros, Th. F., "Adsorption of Poly(vinyl alcohol) on Silica at pH Values and its Effect on the Flocculation of the Dispersion," *Journal of Colloid and Interface Science*, 64(1), pp. 36-47, (1978).
- [Tro83] Tronel-Peyroz, E., Raous, H., and Schuhmann, D., "A Study of the Interfacial behavior of Polyoxyethylene at a Mercury-Aqueous Solution Interface: Compact and Diffuse Layers," *Journal of Colloid and Interface Science*, 92(1), pp. 136-153, (1983).

- [Tsy72] Tsyanenko, A.A., and Filimonov, V.N., "Infrared Spectra of Surface Hydroxyls Groups and Crystalline Structures of Oxides," *Spectroscopy Letters*, 5(12), pp. 477-487, (1972).
- [van 91] van der Beek, G.P., Cohen Stuart, M.A., Fler, G.J., and Hofman, J.E., "Segmental Adsorption Energies for Polymers on Silica and Alumina," *Macromolecules*, 24, pp. 6600-6611, (1991).
- [van 76] van der Marel, H.W., and Beutelspacher, H., "Atlas of Infrared Spectroscopy of Clay Minerals and Their Admixtures," Elsevier Scientific Publishing Company, Amsterdam, The Netherlands, pp. 322-329, (1976).
- [Vas86] Vassilev, K.G., Dimov, D.K., Stamenova, R.T., Boeva, R.S., and Tsvetanov, Ch. B., "Complex Forming Properties of CrossLinked Poly(ethylene oxide). I. Interaction of Linear and CrossLinked Poly(ethylene oxide) with Molybdenum VI Salts," *Journal of Polymer Science:Part A:Polymer Chemistry*, 24, pp. 3541-3554, (1986).
- [Wal96] Walker, W.J., Reed, J.S., Verma, S., and Zirk, W., "Adsorption Behavior of Polyethylene Glycol", Paper No. B-101-96, presented at the 98th Annual Meeting of the American Ceramic Society, Indianapolis, IN, (1996).
- [Wei95] Weissenborn, P.K., Warren, L.J., and Dunn, J.G., "Selective Flocculation of Ultrafine Iron Ore. 1. Mechanism of adsorption of starch onto hematite," *Colloids and Surfaces*, 99, pp. 11-27, (1995).
- [You58] Young, G.J., "Interaction of Water Vapor With Silica Surfaces," *Journal of Colloid Science*, 13, pp. 67-85, (1958).

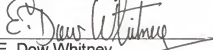
## BIOGRAPHICAL SKETCH

Sharad Mathur was born in Kotputli, India, on December 14, 1966. After completing his primary education at the St. Paul's School, Kota, he entered the bachelor's program in ceramic engineering at the Institute of Technology, Benaras Hindu University, Varanasi, India. He graduated in May 1988 and proceeded to Canada in September 1988 to pursue further studies at McMaster University, Hamilton. After obtaining his M.Eng. degree in materials science and engineering in August 1991, he took a four month hiatus in India. He joined the doctoral research program in the Department of Materials Science and Engineering at the University of Florida in January, 1992.

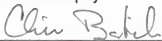
I certify that I have read this study and that in my opinion it conforms to acceptable standards of scholarly presentation and is fully adequate, in scope and quality, as a dissertation for the degree of Doctor of Philosophy.

  
Brij M. Moudgil, Chairman  
Professor of Materials  
Science and Engineering


I certify that I have read this study and that in my opinion it conforms to acceptable standards of scholarly presentation and is fully adequate, in scope and quality, as a dissertation for the degree of Doctor of Philosophy.

  
E. Dow Whitney  
Professor of Materials  
Science and Engineering

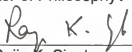
I certify that I have read this study and that in my opinion it conforms to acceptable standards of scholarly presentation and is fully adequate, in scope and quality, as a dissertation for the degree of Doctor of Philosophy.

  
Christopher D. Batich  
Professor of Materials  
Science and Engineering

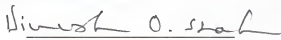
I certify that I have read this study and that in my opinion it conforms to acceptable standards of scholarly presentation and is fully adequate, in scope and quality, as a dissertation for the degree of Doctor of Philosophy.

  
Hassan El-Shall  
Engineer of Materials Science  
and Engineering

I certify that I have read this study and that in my opinion it conforms to acceptable standards of scholarly presentation and is fully adequate, in scope and quality, as a dissertation for the degree of Doctor of Philosophy.

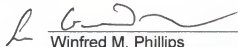
  
\_\_\_\_\_  
Rajiv K. Singh  
Associate Professor of  
Materials Science and  
Engineering

I certify that I have read this study and that in my opinion it conforms to acceptable standards of scholarly presentation and is fully adequate, in scope and quality, as a dissertation for the degree of Doctor of Philosophy.

  
\_\_\_\_\_  
Dinesh O. Shah  
Professor of Chemical  
Engineering

This dissertation was submitted to the Graduate Faculty of the College of Engineering and to the Graduate School and was accepted as partial fulfillment of the requirements for the degree of Doctor of Philosophy.

December 1996

  
\_\_\_\_\_  
Winfred M. Phillips  
Dean, College of Engineering

\_\_\_\_\_  
Karen A. Holbrook  
Dean, Graduate School

LD  
1780  
1996  
.M432

